

Review of Machine-learning Methods for Integrated Renewable Power Generation: A Comparative Study of Artificial Neural Networks, Support Vector Regression, and Gaussian Process Regression

Mahdi Sharifzadeh^{a, b, 1}, Alexandra Sikinioti-Lock, Nilay Shah

^a Department of Chemical Engineering, Imperial College London, South Kensington Campus, London SW7 2AZ, United Kingdom

^b Department of Electronic and Electrical Engineering, University College London, WC1E 7JE, United Kingdom

Abstract

Renewable energy from wind and solar resources can contribute significantly to the decarbonisation of the conventionally fossil-driven electricity grid. However, their seamless integration with the grid poses significant challenges due to their intermittent generation patterns, which is intensified by the existing uncertainties and fluctuations from the demand side. A resolution is increasing energy storage and standby power generation which results in economic losses. Alternatively, enhancing the predictability of wind and solar energy as well as demand enables replacing such expensive hardware with advanced control and optimization systems. The present research contribution establishes consistent sets of data and develops data-driven models through machine-learning techniques. The aim is to quantify the uncertainties in the electricity grid and examine the predictability of their behaviour. The predictive methods that were selected included conventional artificial neural networks (ANN), support vector regression (SVR) and Gaussian process regression (GPR). For each method, a sensitivity analysis was conducted with the aim of tuning its parameters as optimally as possible. The next step was to train and validate each method with various datasets (wind, solar, demand). Finally, a predictability analysis was performed in order to ascertain how the models would respond when the prediction time horizon increases. All models were found capable of predicting wind and solar power, but only the neural networks were successful for the electricity demand. Considering the dynamics of the electricity grid, it was observed that the prediction process for renewable power and wind was fast and accurate enough to effectively replace the alternative electricity storage and standby capacity.

Keywords

Machine-learning, Big Data, Renewable Wind and Solar Power, Electricity demand, Artificial Neural Networks (ANN), Support Vector Regression (SVR), Gaussian Process Regression (GPR).

¹ **Corresponding Author:** Roberts Building, Department of Electronic and Electrical Engineering, University College London, London, UK. WC1E 7JE. **Email:** m.sharifzadeh@ucl.ac.uk

34 **1. Introduction**

35 Nowadays the need to move towards more sustainable technologies and methods is more urgent than ever due to
36 the adverse effects caused by climate change. The International Energy Agency [1] asserts that over 65% of the
37 GHGs (greenhouse gases) emanate from the energy sector, which signifies the need for transformation within this
38 sector. Recent global events such as COP21 have set challenging targets to prevent the alarming impacts of climate
39 change, which will be addressed by the adoption of stringent legislation. While the power sector accounts for 66%
40 of the GHG emissions globally [1], renewable energy resources (RESs) have a burgeoning leading role in its
41 decarbonisation. However, the intermittent generation patterns of solar and wind power due to the meteorological
42 effects have rendered their deep implementation difficult, and further research and measures are required. In an
43 electricity grid, the primary objective is to ensure the balance between supply and demand, in order to avoid power
44 cuts and ensure that all consumers receive the electricity they need. This can be met by installing energy storage
45 units as well as the commitment of stand-by generation capacities, but such an integration raises the costs of the
46 electricity grid.

47 For this reason, many endeavours have been made in predicting power load as well as electricity generation from
48 RESs, which with sufficient accuracy could minimise operational costs and facilitate their technological
49 penetration [2]. One of the approaches with which this issue is addressed is by enhancing the near-term
50 predictability of the renewable energy systems and incorporating this knowledge into smart control systems that
51 can optimise the power dispatch within an electricity smart grid. Here Big Data analytics is the “enabler” as it can
52 convert real-time data, into “actionable knowledge”. Many studies have been conducted with the view to
53 predicting the renewable energy generation as well as the electricity demand. Extensive reviews can be found for
54 the prediction of electricity demand [3,4], the photovoltaic power generation in [5], [6] and the wind power [7].
55 Baños et al., [8] reviewed the optimisation studies focused on all areas of renewable energy operation. Here, the
56 broad observation is that artificial intelligence methods tend to outperform the respective statistical approaches
57 [9–11]. These application areas are briefly reviewed in the following.

58 **1.1. Predicting power generation from wind energy**

59 Wind power forecasting has had a growing interest in the research community throughout the last decades [12].
60 Research involving forecasting wind power generation is summarized in **Table 1**. In [13] an extensive review is
61 provided on the feature selection methodologies that have used across the literature for wind power prediction. It
62 was additionally shown that feature selection is an important pre-processing technique when using AI techniques.

63 Two trends can be found in the literature for wind power forecasting in which the wind power is either predicted
64 directly from historical data and wind speed, or indirectly by predicting wind speed and converting the speed to
65 power via power curves. A review was conducted that groups the studies accordingly [14]. Shi, et al. [15]
66 conducted a comparative study between predicting the wind power directly from the historical data and indirectly
67 from power curves and found that wind speed data provides better accuracy. They showed that the former method
68 produces more accurate results, which is expected since the correlation between wind speed and power is
69 stochastic and cannot satisfy a deterministic approach. The inability to predict wind power with the use of power
70 curves is also discussed in [16,17]. Meng et al. [18] applied a hybrid method where wavelet packet decomposition
71 was first applied for pre-processing wind data and their decomposition into time subseries, which are then using
72 for training an artificial neural network (ANN) using a crisscross optimization algorithm. It was observed that the
73 proposed algorithm outperforms other methods for 1 to 5-hour ahead predictions. In addition, outperformed back-
74 propagation and particle swarm optimization in training the ANN parameters. Similarly, Liu et al. [19] applied a
75 hybrid method consisting of wavelet transformation and two neural networks. The decomposed low-frequency
76 sub-layers of wind speed data was applied for training a long short-term memory neural network, and the high-
77 frequency sub-layers were applied for training an Elman neural network. Wang et al. [20] applied a similar hybrid
78 algorithm in which wavelet transform was applied to decompose the signals into various frequency series. The
79 data sets were then applied for training a deep belief network, where the uncertainties was handed by the spine
80 quantile regression. Huai-zhi et al. [21] applied a deep learning based ensemble framework that was a combination
81 of wavelet transform and convolutional neural networks. They demonstrated the success of their approach on case
82 studies from China. Yu et al. [22] proposed a hybrid approach in which the data is decomposed into time series
83 using a Gaussian mixture copula method, and then applied for training Gaussian process regression models. The
84 proposed method showed promise in accommodating seasonality variations, and uncertainties in the wind speed.
85 The performance of linear, non-linear, artificial intelligence and hybrid models for predicting the mean hour-wind
86 speed was examined with comparison to one another in [9]. More specifically, AR, ARIMA, MLP, RBF, ELM,
87 ANFIS, and NLN models were built and it was concluded that linear models had the largest errors, whereas the
88 non-linear and artificial intelligence (AI) models had approximately close errors with the neural network logic
89 having the lowest. Yu et al. [23] applied an improved neural network structure called Long Short-Term Memory-
90 enhanced forget-gate (LSTM-EFG), combined with Spectral Clustering to extract temporal correlation
91 characteristics for forecasting wind power. The authors reported up to 18.3% higher accuracy compared to
92 conventional LSTM, SVR, and KNN methods with higher computational efficiency. Liu et al. [24] applied a

93 model consisting of three elements; wavelet packet decomposition (WPD) was applied for decompose the original
94 time-series into several sublayers. The high frequency sublayer was to train a convolutional neural network (CNN)
95 with a one-dimensional convolution operator. Finally, a convolutional long short term memory network
96 (CNNLSTM) was applied for low frequency sublayers. The author reported superior performance and robustness
97 against sudden changes in the wind speed. Similar studied by Liu et al. [19,25], using the same strategy for
98 decomposing the data to multilayers and training various recurrent neural networks, which showed improvements
99 over conventional approaches. Zhu et al. [26] applied convolutional neural networks for four-hours ahead forecast
100 of wind farm with successful results. Hu and Chen [27] applied a nonlinear hybrid model in which, hysteresis (a
101 biological neural system property) was included in the activation function to improve the performance of an
102 Extreme Learning Machine (ELM) model. In addition, a weighted objective function was optimized using
103 Differential Evolution algorithm (DE) in order to establish the balance between “learning performance” and
104 “model complexity” in a long short term memory neural network (LSTM). The authors reported superior
105 performance over other conventional models for the cases of the ten-minute ahead (utmost short term) and one-
106 hour ahead (short term) wind power predictions. Wang and Li [28] developed a model consisting of the three
107 elements of optimal feature extracting, deep learning and error correction for wind speed prediction. The feature
108 extraction element consisted of variational mode decomposition, Kullback-Leibler divergence, energy measure
109 and sample entropy methods. A long short term memory (LSTM) network was applied for deep learning. A
110 generalized auto-regressive conditionally heteroscedastic model was applied for error correction. The
111 demonstrated the superior performance of the model over benchmarks using three sets of real data. Wang et al.
112 [29] used k-mean clustering for the classification of numerical weather prediction (NWP) data, which was then
113 applied for training a deep belief network (DBN) consisting of cascading restricted Boltzmann machines (RBMs).
114 The authors validated their model using data from the Sotavento wind farm in Spain. The results demonstrated
115 more than 44% improvement over a back-propagation neural network (BP) and a Morlet wavelet neural network
116 (MWNN) benchmark. Zhang et al. [30] studied short-term wind power forecaster, using a hybrid model. Singular
117 spectrum analysis was applied to decompose the original data into a trend component and a fluctuation component.
118 The trend component was forecasted using a least squares support vector machine, while the fluctuation
119 component was predicted using a deep belief network (DBN). A locality-sensitive hashing search algorithm was
120 applied to cluster the nearest training samples for further improvement.

121 Yu et al. [31] developed three hybrid models include wavelet transform is firstly adopted to decompose the data
122 into several sub-series. The second element of the model included either a standard recurrent neural network

123 (RNN), a long short term memory (LSTM) neural network, or a gated recurrent unit neural (GRU) network aimed
 124 at extracting “deeper features”. The final element consisted of support vector machine (SVM) for prediction. The
 125 authors demonstrated the performance of their hybrid methods using real data. Higashiyama et al. [32] applied
 126 feature extraction from numerical weather prediction (NWP) data using three-dimensional convolutional neural
 127 networks (3D-CNNs) which has the advantage of direction extraction of spatio-temporal features from NWP data.
 128 They demonstrated the superior performance of their model against benchmark models. Chen et al. [33] applied
 129 a hybrid model based on support vector regression machine (SVRM), Long Short Term Memory neural networks
 130 (LSTMs), and an extremal optimization algorithm (EO) for forecasting wind speed. A cluster of LSTMs was
 131 applied to explore the implicit information of wind data. Then, the parameters of the nonlinear SVRM model were
 132 optimized using the extremal optimization algorithm. The demonstrated the performance of their model for 10min
 133 ahead prediction of wind speed data from inner Mongolia, China.

134 In [16], between 4 different data mining algorithms, namely support vector regression (SVR), the multilayer
 135 perceptron (MLP), and two types of regression trees the accuracy of the SVR was the highest. Chen et al. [34]
 136 reported that dynamical GPR (Gaussian Regression Process) outperforms an MLP (Multilayer Perceptron Neural
 137 Network). Jiang et al. [35] also observed that GPR displayed good performance in comparison to MLP and SVM
 138 (Support Vector Machine) for predicting the wind speed. In the study by Ernst et al. [36], SVM yielded the best
 139 predictions out of artificial neural networks (ANN), a mixture of experts (ME) and nearest neighbour search
 140 (NNS) for wind power. However, when all the models were incorporated together as an ensemble model the least
 141 errors were achieved. It has been observed that the combination of multiple modelling techniques could optimise
 142 the performance of the predictions [37,38], since the weaknesses observed in some models may be smoothed by
 143 others. Tascikaraoglu and Uzunoglu provide an extensive review of the ensemble methodologies that have been
 144 used for wind power forecasting [39]. Finally, accuracy measures and benchmarking techniques used in the
 145 literature have been reviewed by [7,40].

146

147 **Table 1.** Literature concerning wind speed and power forecasting

| Authors | Input (historical data) | Output (predictions) | Forecast horizon | Method | Models used |
|---------------------------|---|----------------------|------------------|-------------------------|-------------|
| Ak, Vitelli and Zio, [41] | Wind Speed | Wind Speed | Short-term | Statistical | MLP |
| Masseran [42] | Wind Speed | Wind Speed | Short-term | Statistical | ARIMA ARCH |
| Shi, Qu and Zeng [15] | NWP, Wind Power | Wind Power | Short-term | Statistical | ARIMA |
| Alexiadis [43] | Wind Speed, Direction, Pressure, Temperature, Spatial correlation | Wind Speed and Power | Very short-term | Artificial Intelligence | ANN, ARMA |

| | | | | | |
|---------------------------------------|---|----------------------|--------------------------------|-------------------------|---|
| Sideratos and Hatziaargyriou [44] | Wind Power, NWP time series | Wind Power | Short-term | Artificial Intelligence | RBF, FLS |
| Mohandes et al.[45] | Daily Mean Wind Speed | Wind Speed | Long-term | Artificial Intelligence | SVM, MLP |
| Jursa and Rohrig [46] | Wind Power, NWP time series of multiple areas | Wind Power | Short-term | Artificial Intelligence | ANN/kNN |
| Ghadi et al. [47] | NWP, SCADA | Wind Power | Short-term | Artificial Intelligence | ICA, ANN |
| Kramer and Gieseke [48] | Wind Speed | Wind Power | Short-term | Artificial Intelligence | SVR |
| Han, Li and Liu [49] | Wind Speed Direction, Air Temperature, Air Pressure, Relative Humidity | Wind Power | Short-term | Artificial Intelligence | ANN |
| Carolin Mabel and Fernandez [50] | Wind Speed , Relative Humidity, Generation Hours Energy Output | Wind Power | Short-term | Artificial Intelligence | ANN |
| Cellura et al. [51] | Weibull Distribution | Wind Speed | Short-term | Artificial Intelligence | ANN, Universal kriging (UK) estimator |
| Welch, Ruffing and Venayamoorthy [52] | Wind Speed, Temperature, Relative Humidity | Wind Speed | Short-term | Artificial Intelligence | ANN (MLP, ELM, SRN) |
| Ernst et al., [36] | Wind Power, NWP time series of multiple areas | Wind Power | Short-term | Artificial Intelligence | SVM, ANN, ME, NNS (ensemble) |
| Ramirez-Rosado et al. [53] | NWP, Wind Power | Wind Power | Short-term | Hybrid | MLP/Kalman-ARIMA-FLS |
| Bin, Haitao and Ting [54] | Historic Wind Speed | Wind Speed | Short-term | Artificial Intelligence | NN, GPR, LS-SVR |
| Hong, Pinson and Fan [55] | Historic Wind Power | Wind Power | Short-term | Artificial Intelligence | NN, GPR, SVM |
| Jiang et al. [35] | Historic Wind Speed | Wind Speed | Short-term | Artificial Intelligence | GPR |
| Chen et al. [34] | NWP | Wind Power | Short/medium terms | Artificial Intelligence | GPR, ANN |
| Sfetsos, [9] | Hourly Wind Speed | Hourly Wind Speed | Short-term | Statistical, Hybrid | NLN, AR, ARMA, ANFIS, RBF |
| Kusiak, Zheng, and Song [16] | Wind Speed and Power | Wind Speed and Power | Short-term | Hybrid | SVM(speed), kNN(power) |
| Barbounis and Theocharis [56] | Spatial Correlation, Wind Speed Data | Wind Speed | Very short-term | Hybrid | FNN |
| Hu et al. [37] | Wind Power | Wind Power | Very short term (15m) | Hybrid, ensemble | ARIMAX, bagging, QRF, RF, QR-SVM, QR-NN |
| Barbosa de Alencar et al. [38] | Air Temperature, Air Humidity, Atmospheric Pressure, average wind speed, wind direction | Wind Speed | Very Short/Short./Medium /Long | Hybrid, ensemble | NN, ARIMA |
| Eseye et al. [57] | NWP | Wind Power | Medium-term | Artificial Intelligence | GA-ANN, BP NN |
| Najeebullah et al. [58] | Wind Speed, Relative Humidity, Temperature | Wind Power | Medium-term | Hybrid | ANN, SVR |
| Li et al. [59] | NWP | Wind Power | Short-term | AI | SVM |

148

149 1.2. Predicting power generation from solar energy

150 With respect to the input selection for solar power forecasting, data from numerical weather predictions (NWP)

151 and historic power production are used in most cases. The research in the field is summarized in **Table 2**. Bacher

152 et al. applied two autoregressive models for PV power forecasting in which both had an input of the historic power
153 production data, but only one of them used additionally NWP. It was concluded that the model which used the
154 NWP had a better performance particularly for predictions after two hours, but for very short-term predictions,
155 historical data was the most vital entry [60].

156 Artificial intelligence and statistical methods have been implemented for solar irradiance and photovoltaic power
157 predictions extensively in various comparative studies, with a view to identifying the methods that fit better to
158 this application. The applied methods are very diverse and include auto-regressive time-series [60], regression
159 trees [61], k-nearest neighbours (kNNs) [62,63], artificial neural networks (ANNs) [64,65], support vector
160 regression [66,67], and Gaussian process regression [68] to name a few. Martín et al. [10] found that multilayer
161 neural networks (MLP) and adaptive neuro-fuzzy inference systems (ANFIS) are superior in predicting the solar
162 energy that is harnessed by solar thermal plants compared to autoregressive statistical models. Salcedo-Sanz et al.
163 [69] studied the prediction of the total daily solar irradiance with a number of various techniques, such as SVR,
164 ELM, Bagged Trees and GPR and found that GPR had a better accuracy than other methods. Fernandez-Jimenez
165 et al. [11] compared various statistical and AI models namely kNN, ANFIS, ARIMA and ANN (MLP, EML,
166 RBF), where data was obtained from two different numerical weather (NWP) prediction programmes. It was
167 shown that the MLP ANN outperformed all the other models followed by ANFIS. Similarly, in [62] MLP neural
168 networks were successful in making 1 hour and 2 hour forecasts with the use of historical data of power produced
169 by a PV farm compared to the statistical method ARIMA and the kNN. For small time steps (5 minutes), Reikard
170 [70] found that ANN provided more accurate forecasts compare to an ARIMA method as well as from a hybrid
171 method of ANN coupled with ARIMA. On the other hand, for larger time steps, the ARIMA was the best method
172 (15, 30, 60 min). This is expected since on higher resolutions the forecast is more data dependent making the
173 ANN the better choice, whereas for lower resolutions the diurnal cycle can be captured more effectively by
174 regression methods. Behera et al. [71] applied a single layer feed-forward whose weights were optimized using a
175 particle swarm algorithm. Sharma and Kakkar [72] applied four machine-learning tools, namely FoBa,
176 leapForward, Spikeslab, Cubist and bagEarthGCV for predicting solar irradiance. The underlying methodologies
177 of these models were an adaptive forward-backward greedy algorithm, regression subset selection algorithm, a
178 spikes and slab algorithm, a rule-based multivariate linear modelling, a multivariate adaptive regression splines
179 algorithm, respectively. The results of Spikeslab and Cubist were reported to be stable and accurate for different
180 time horizons. Tang et al. [64] applied a combination of extreme learning machine and entropy method. They
181 reported that this hybrid algorithm performs better than a generalized regression neural network, and a radial basis

182 function neural network, for short-term photovoltaic power forecast. Similarly, Hossain et al. [73] applied an
183 extreme learning machine (ELM) algorithm for predicting power output from a photovoltaic system. They
184 reported a superior performance compared to SVR and ANN benchmarks. Majumder et al. [74] applied
185 Variational Mode Decomposition and Extreme Learning Machine for predicting solar irradiation. The algorithm
186 was reported robust under noisy conditions and despite the presence of outliers in the historical data. Srivastava
187 and Lessmann [75] studied the forecast of forecasting global horizontal irradiance (GHI), a measure of shortwave
188 radiation received used for PV installation, using a long short term memory (LSTM) neural network. The average
189 forecast skill of 52.2% over benchmark was reported. Qing and Niu [76] applied LSTM neural networks for hourly
190 day-ahead solar irradiation prediction from weather data. Using experimental data, they demonstrated 18.34 and
191 42.9% improvements in root mean square error (RMSE), compared to BPNNs, for two datasets. Alzahrani et al.
192 [77] applied deep recurrent neural networks (DRNNs) for forecasting solar irradiance, using real data from
193 Canada. They demonstrated significant improvements over conventional methods such as support vector
194 regression (SVR) models, and feedforward neural networks (FNNs). Li et al. [78] studied short-term solar power
195 forecast. Using correlation coefficient, they identified the solar radiation intensity, atmospheric temperature and
196 relative humidity as the most correlated variables with the photovoltaic power output. A deep belief network was
197 applied which should significant improvements over a base-line back propagation (BP) neural network. Abdel-
198 Nasser and Mahmoud [79] applied long short-term memory recurrent neural network (LSTM-RNN) to forecast
199 solar power generation. Compared to multiple linear regression (MLR) model, bagged regression trees (BRT),
200 and feedforward neural network models, their LSTM-RNN model showed a superior performance. Zhang et al.
201 [80] studied several ANN configuration for short term (in the order of minutes) of photovoltaic power generation,
202 namely multi-layer perceptron (MLP), convolutional neural network (CNN), and long short term memory (LSTM)
203 structures. Image data such as the sun intensity, cloud movement and appearance, was applied to forecast the
204 solar power generation. The authors report root mean squared error (RMSE) of 7%, 12% and 21% for the MLP,
205 LSTM, and CNN configurations, respectively. Wang et al. [81] applied hybrid deterministic and probabilistic
206 models for forecasting photovoltaic power. The deterministic model consisted of wavelet transform (WT) and
207 deep convolutional neural network (DCNN). WT was applied for decomposing original signal into several
208 frequency series which were applied for training the DCNN model. The probabilistic model was developed by
209 extending the deterministic model using spine quantile regression (QR). They demonstrated the outperformance
210 of their method using real data from PV farms in Belgium.

211
212

Table 2. Literature concerning solar irradiance and PV power forecasting

| Authors | Forecast horizon | Method Type | Method | Prediction Output | Input |
|--------------------------------------|------------------|---------------------------------|---------------------------------------|---|--|
| Ridley, Boland and Lauret [82] | Short-term | Statistical | BIC | Diffuse solar radiation | Hourly/Daily Clearness index, Solar altitude, Apparent solar time, Measure of persistence of global radiation levels |
| Ruiz-Arias et al. [83] | Short-term | Statistical | AR | Solar Irradiance | Global, diffuse solar radiation |
| Bacher, Madsen and Nielsen, [60] | Short-term | Statistical | AR | PV power | NWP, Past power production |
| Chen et al., [84] | Medium | Artificial intelligence | RBF ANN | PV power | Past power production, NWP (Solar Irradiance, Temperature, Relative Humidity) |
| İzgi et al. [85] | Very short-term | Artificial intelligence | MLP ANN | PV power | Past power production, Solar Irradiance, Temperature, Relative Humidity |
| Mellit and Pavan [86] | Short-term | Artificial intelligence | MLP ANN | Solar Irradiance | Solar Irradiance, Temperature |
| Mellit, Benghanem and Kalogirou [87] | Short-term | Artificial intelligence | MLP ANN | PV power | Solar Irradiation, Temperature, Relative Humidity |
| Mellit et al. [88] | Short-term | Artificial intelligence | FNN | Solar Irradiance | Air Temperature, Relative humidity, Direct, Diffuse Global irradiance, Sunshine duration |
| Martín et al. [10] | Medium | Artificial intelligence | AR, ANN, ANFIS | Solar Thermal Plants | Ground Solar Radiation (hourly), Clearness index, Lost component |
| Shi et al. [89] | Short-term | Artificial intelligence | SVM with weather classification | PV power | NWP, Past power production |
| Yona et al. [90] | Short-term | Artificial intelligence | ANN (MLP, RBF, ELM) | PV power | Global Solar Radiation, Temperature, Atmospheric pressure, Humidity, Cloud amount, Wind speed, and Rainfall |
| Ding, Wang and Bi [91] | Short-term | Artificial intelligence | ANN | PV power | Past power production, Meteorological Data |
| Salcedo-Sanz et al. [69] | Short-term | Artificial Intelligence | ELM, SVR, GPR, Bagged Trees | Solar Irradiance | NWP |
| Sfetsos and Coonick [92] | Short-term | Artificial intelligence, Hybrid | ANN (MLP, ELM, RBF), ANFIS, ARMA | PV power | Solar Radiation, Time indicator |
| Reikard [70] | Short-term | Artificial intelligence, Hybrid | ARIMA, ANN, ARIMA-ANN | Solar Irradiance | Solar Irradiation, Temperature, Relative Humidity, Cloud cover |
| Mellit et al. [93] | Medium | Artificial intelligence, Hybrid | ANFIS, ANN (MLP, RBF) | Mean monthly clearness indexes, daily solar radiation | Latitude, Longitude, Altitude |
| Fernandez-Jimenez et al. [11] | Short-term | Hybrid | kNN, ANN (MLP, RBF,ELM), ANFIS, ARIMA | PV power | Year moment, Past power production, NWP (x2) [Solar power surface sensible heat flux, Surface latent heat flux, Surface downward shortwave radiation, Surface downward longwave radiation, Top outgoing shortwave radiation, Top outgoing longwave radiation, Temperature] |
| Pedro and Coimbra [62] | Short-term | Hybrid | GA-ANN, ANN, ARIMA, kNN | PV power | Past power production |

214 Several of the studies presented in Table 2 have applied various types of artificial neural networks with the view
215 to determining the most suitable one. As mentioned above, Fernandez-Jimenez et al. found that the MLP neural
216 network outperformed ELM and RBF architectures [11]. However, in [90] ELM networks are suggested for time
217 series data forecasting since they exceeded the performance of both the MLP and RBF neural networks. In
218 addition, in [52] it was similarly established that recurrent architectures (ELM) provide a better performance than
219 the respective linear ones (MLP). Finally, Shi et al. implemented Support Vector Machines (SVM) along with a
220 data classification algorithm that categorises days as sunny, foggy, cloudy and rainy and found promising results
221 particularly for the two former categories [89].

222 **1.3. Predicting power demand**

223 Predicting electricity load has been the focus of intense research too. The conducted research is inherently
224 multifaceted, and include input selection, predictive model type and structure, training algorithm, dynamic
225 learning, and the implications of electricity deregulation for the price [94]. **Table 3** summarises the research in
226 the field. Broadly speaking, the prediction horizon can be divided into very short-term, short-term, mid-term and
227 long-term, each with a different set of decision variables (**Table 1**). Amongst these, short-term (hours to a day)
228 prediction of electricity demand has significant implication for the optimal operation of electricity grids, as it has
229 similar time-scale when significant fluctuations occur during stochastic wind and solar power generation. Overall,
230 with regard to the inputs used for demand forecasting, historical load data is essential and in some cases,
231 meteorological information is utilised. The former is of greatest significance in very short-term forecasting (10-
232 30 minutes), whereas for greater time intervals the weather data becomes increasingly important [95]. For
233 instance, Drezga and Rahman studied the optimal variables selection for short-term load forecast using the so-
234 called phase-space embedding method. The input variables applied for training the neural network included
235 electricity load, temperature, as well as daily and half-daily cycles, at different time intervals. They demonstrated
236 that with appropriate selection of only 15 inputs, high accuracy could be achieved for predicting power load on
237 working days and weekends [96]. Sovann et al. [97] applied Autocorrelation (ACF), partial autocorrelation
238 (PACF), and cross-correlation (CCF) in order to identify the best-suited input variables for the neural network-
239 based forecast of electricity load. They reported that a combination of time indicators, lagged load, and weather
240 variables such as dry bulb and dew point temperature provided the best performance. Tao *et al.* [98], proposed a
241 method based on correlation clustering. The idea is that assigning consumers with similar demand behaviour can
242 improve the overall demand forecast. Recently, nonconventional variables were proposed for power consumption

243 prediction. For instance, Vinagre et al. [99] demonstrated that solar radiation serves as a good indicator of energy
 244 consumption for in a building.

245

246 **Table 3.** Literature concerning demand forecasting

| Authors | Forecast horizon | Method Type | Method | Input |
|---------------------------------------|-------------------------|-------------------------|---------------------|--|
| Taylor [100] | Short-Term | Statistical | ARMA, EXS | Historic Load Data |
| Taylor, de Menezes and McSharry [101] | Short-Term | Statistical | EXS, PCA | Historic Load Data |
| Taylor and Buizza [102] | Short-Term | Statistical | ARMA | Historic Load Data, NWP, Weather data |
| Gould et al. [103] | Short\Medium Term | Statistical | EXS | Historic Load Data |
| Al-Hamadi and Soliman [104] | Short-Term | Statistical | Kalman Filtering | Historic Load & Weather Data, Current Weather Data |
| Taylor and Mcsharry [105] | Short-Term | Statistical | ARIMA, AR, EXS, PCA | Historic Load Data |
| Taylor [95] | Very short-term | Statistical | ARIMA, AR, EXS, PCA | Historic Load Data |
| Villalba and Alvarez [106] | Short-Term | Artificial Intelligence | ANN | Historic Load Data |
| Wang et al. [107] | Short-Term | Artificial Intelligence | ϵ -SVR | Historic Load Data |
| Zheng, Zhu and Zou [108] | Short-Term | Artificial Intelligence | SVM | Historic Load Data |
| Badri, Ameli and Motie Birjandi [109] | Short-Term | Artificial Intelligence | ANN, FLS | Historic Load Data |
| Ho et al. [110] | Short-Term | Artificial Intelligence | ES | Historic Load & Weather Data |
| Galarniotis et al. [111] | Short-Term | Artificial Intelligence | ELM, FIR | Historic Load Data |
| Hong, Pinson, and Fan [55] | Short-Term | Artificial Intelligence | ANN, GPR | Historic Load Data, Temperature |
| Shu and Luonan [112] | Short-Term | Hybrid | SOM-SVM | Historic Load Data |
| Zhang and Dong [113] | Short-Term | Hybrid | ANN-Wavelet | Historic Load Data |
| Song et al. [114] | Short-Term | Hybrid | FLS | Historic Load Data |

247

248 The examples of the machine-learning methods applied for load forecast include time series [115], linear
 249 regression [116], moving average [117], wavelet transforms [118], support vector regression (SVR) [119],
 250 Gaussian process regression (GPR) [120], Fuzzy models [121], Artificial Neural Networks (ANNs) [94], and
 251 expert systems [122,123]. Artificial neural networks have been broadly used for demand forecasting. Hippert, et
 252 al. [124] presented a review of the load forecasting methods. In [111,125], a comparative study was conducted
 253 with regard to the MLP, FIR and ELM neural networks. It was established that ELM and FIR are more capable
 254 in forecasting time series than MLP, with the latter of the two producing the best results. It should be mentioned
 255 that neural networks outperform FL models due to their ability to compute nonlinearity in the data [109]. Support
 256 Vector Machines and Regression have also been extensively used in load forecasting [107,108,112]. Support

257 vector regression was applied to a smoothed and pre-processed dataset of the load corresponding to East China,
258 the results of which were further developed in order to account for the seasonal variations [107]. Three different
259 Support Vector Machines were compared in [108], namely a Gaussian wavelet SVM, a conventional Gaussian
260 SVM and a Morlet wavelet SVM, and it was found that the former had a superior performance both in accuracy
261 and speed. Hong et al. [55] reported a forecasting competition where several techniques were considered in order
262 to forecast the load for a number of different horizons by using historical data and temperature information.
263 Amongst the various methods developed, GPR was found the best in terms of accuracy. Almehaiei and Soltan
264 [117] proposed a method based on decomposition and segmentation of the electricity time series for daily load
265 forecast. They demonstrated their method on a case study from Kuwaiti electric network. Outliers in historical
266 load data could severely degrade the accuracy of forecast. With the view of overcoming this challenges, Zhang et
267 al. [126] proposed a method based on spatial-temporal feature clustering, and demonstrated its effectiveness. What
268 is more, the volume of data has an impact on the accuracy of the forecasting models; when sufficient data on load
269 was provided that could represent not only the weekly and daily patterns but also the respective annual ones, the
270 accuracy of the statistical model used (ARMA) increased significantly [100]. With a view to establishing the most
271 suitable statistical methods, a comparative study was carried out by Taylor and McSharry and it was found that
272 exponential smoothing outperformed the ARIMA, AR, and PCA models [105]. Coelho et al. [121] proposed a
273 hybrid model with adaptive parameter update using an evolutionary bio-inspired optimization algorithm. They
274 described the method computationally efficient and accurate for predicting short-term electricity load. Hong [127]
275 applied a hybrid method consisting of recurrent neural networks (RNNs), support vector regression (SVR), chaotic
276 artificial bee colony algorithm. Such hybrid algorithm offers several desirable functionalities such as seasonal
277 classification and adjustment, recurrent calculations, and chaotic sequence to enable seasonal and monthly
278 electricity forecast. Dedinec et al. [128] applied a deep belief network (DBN) consisting of multiple layers of
279 restricted Boltzmann machines for forecasting electricity load. The author demonstrated the performance of their
280 method using real data from the Macedonian system operator (MEPSO), which showed between 8.6% to 21%
281 reduction in the absolute percentage error (MAPE) compared to a typical feed-forward multi-layer perceptron
282 neural network. Shi et al. [129] applied a deep learning algorithm for the two power load forecast of aggregated
283 demand in New England, and 100 individual households in Ireland. They reported up to 23% improvements in
284 the aggregated case and 5% improvement in the disaggregated case compared to a “shallow neural network”
285 benchmark.

286 Hernández et al. [130] applied a multi-agent architecture based on multi-layer perceptrons (MLP) neural network,
287 in the context of virtual power plants for collaborative load forecast. Javed et al. [131] proposed a multiple load
288 forecasting model which combines individual time-series into a single model, using ANNs and SVMs. They
289 demonstrated that such aggregated model is superior for predicting short-term demand. Critical reviews of demand
290 forecasting, dynamic pricing and demand side management is recently presented by Khan et al. [4], Raza *et al.*
291 [94], and Hernandez et al.[132].

292 A close research area is concerned with the electricity price forecasting. In a deregulated market, this price is
293 closely related to the deficit and surplus between supply and demand. By the emergence of renewable power from
294 wind and solar, the electricity supply-demand balance has become more and more uncertain. Therefore, the
295 electricity price forecast has been the subject of intensive research. While a comprehensive review of these
296 methods is beyond the scope of this article, Weron and Nowotarski have provided extensive reviews and recent
297 updates [133,134] for electricity price forecasting. More recent studies have focused on hybrid methods. Yang et
298 al. [135] applied the kernel extreme learning machine (KELM) and autoregressive moving average (ARMA) for
299 forecasting electricity price. The parameters of KELM are optimized using a particle swarm optimization
300 algorithm and therefore, the overall framework is self-adaptive. The performance of the method was demonstrated
301 on a few case studies from the US, Spain, and Australia. Inspired by the field of chemical reaction optimization,
302 Abedinia et al. [136] proposed a combinatorial neural network (CNN) framework, in which the parameters of
303 CNN are optimized by a stochastic search algorithm. Wang et al. [137] developed a hybrid framework based on
304 empirical mode decomposition, variational mode decomposition, and neural networks. The developed method
305 proved efficient for multi-step prediction of the electricity prices in several case studies from France and Australia.
306 Amjady and Daraeepour [138] proposed that due to the interrelation between the electricity demand and price, it
307 is more effective to forecast them simultaneously. They applied mutual information (MI) for the selection of
308 inputs, and a cascaded neuro-evolutionary algorithm for learning. Ghasemi et ai, [139] for forecasting electricity
309 price and load. They applied a hybrid algorithm in which Conditional Mutual Information (CMI) and adjacent
310 features were applied for input selection. The input signals were decomposed into several terms using Flexible
311 Wavelet Packet Transform (FWPT). Finally, nonlinear least square support vector machine (NLSSVM) and
312 autoregressive integrated moving average (ARIMA) were applied for learning.

313 The above-mentioned artificial neural network models fall in the category of deterministic machine-learning
314 methods. In the recent years, the deterministic methods are developed further to include the confidence intervals
315 of predictions too, known as probabilistic forecasting methods. The probabilistic forecasting methods could be

316 based on scenario with assigned probability, or in the form of probabilities of quantiles, intervals, or density
317 functions [140]. While thorough review of these methods are not in the scope of the present publication, interested
318 readers are referred to recent reviews by Hong and Fan [140], Zhang et al. [141], and van der Meer and
319 Munkhammar [142].

320 Finally, it should be noted that the application of forecasting method is gaining wide-spread acceptance in power
321 and energy industry. Examples of lateral application include occupancy prediction of office buildings [143], State
322 of charge estimation for electric vehicle [144] the estimation of energy consumption in buildings using solar data
323 [145], and forecasting the of district heating consumption [146], security assessment of power systems [147], and
324 restoring microgrids after fault occurrence [148].

325 Despite the broad research in the literature, a comprehensive analysis where the performance of all the key
326 machine-learning algorithms is compared against a consistent set of data is missing. The key contribution of this
327 study is to exhaustively compare the three machine-learning methods of ANN, GPR, and SVR against a
328 comprehensive set of solar, wind and demand data, hence illustrating the challenges that need to be overcome and
329 quantifying the performance of each method.

330 In the first part of this publication, an introduction was presented that puts the research in context. The next section
331 outlines the methodology that was followed throughout this research, starting with the data pre-processing steps
332 that were required prior to performing any prediction, and continuing with the exact procedures with which the
333 predictive models were tuned and built. The third section will present the results and is split into five categories,
334 namely wind power prediction, solar power prediction, electricity demand prediction and the comparison of
335 results. The final section summarizes the observations and proposes future research directions.

336 **2. Methodology**

337 The research methodology is presented in two parts. The first part describes the data acquisition and pre-
338 processing. The second part reports the employed machine-learning algorithms and their implementation methods.
339 More details are provided in the online Supplementary Materials.

340 **2.1. Data pre-processing**

341 As the objective of this research was to develop data-driven models that can produce relatively accurate
342 predictions for the wind power, solar power, and electricity demand, the acquisition, and processing of data is one
343 of the most important aspects of the present research, to which special attention is paid. In the next subsections
344 the data that was used in this study will be introduced, followed by an elaboration on the procedures that were
345 implemented with regard to its processing. More specifically, the topics of normalisation, cleaning, time series

346 data clustering, and correlation analysis will be covered. The former two are procedures which are more often
 347 than not implemented with every data training technique, and are to large extent common for data pre-processing.
 348 Data clustering was required specifically for the electricity demand, in order to construct the training datasets.
 349 Finally, the correlation analysis was one of the most important parts of the present research, as it provided an
 350 insight for the lags that were used by the predictive NARX models.

351 **Table 4** summarizes different inputs available in the present study, for each type of model training and validation,
 352 more specifically, the data used for wind power prediction included the wind power, the wind speed at 10m above
 353 ground level at the specific location, and the temperature. For the solar power prediction, the inputs include direct
 354 and diffuse irradiance, as well as the temperature. Finally, the only information applied for the demand is the
 355 hourly measurement of consumed electrical energy per household.

356 **Table 4.** Inputs used for wind power, solar power, and electricity demand forecasting.

| Input Vectors | Wind Power Prediction | Solar Power Prediction | Electricity Demand Prediction |
|-------------------------------------|-----------------------|------------------------|-------------------------------|
| Hourly Variable | ✓ | ✓ | ✓ |
| Seasonal Variable | ✓ | ✓ | ✓ |
| Wind Power (KW) | ✓ | | |
| Solar Power (KW) | | ✓ | |
| Electricity Energy [Wmin] | | | ✓ |
| Temperature (°C) | ✓ | ✓ | |
| Wind Speed at 10m ($\frac{m}{s}$) | ✓ | | |
| Direct irradiance (KW) | | ✓ | |
| Diffuse irradiance (KW) | | ✓ | |

357 The wind and solar data were acquired from the ninja renewables website [149] and the details that were input
 358 can be observed in **Table 5**. Here, the location shown corresponds to a southeast location of the UK, namely
 359 Canterbury. For the wind simulations, one of the most commonly used onshore wind turbines was used, a Vestas
 360 V80 [150,151]. The dataset covered the years from 1985 to 2014.

362 **Table 5.** The option used for the ninja renewables simulations

| Required details for simulation | Values |
|---------------------------------|-----------------|
| Latitude [°] | 51.379 |
| Longitude [°] | 1.441 |
| Wind turbine capacity [kW] | 1 |
| Wind Turbine Hub Height [m] | 58 |
| Wind Turbine Model | Vestas V80 2000 |
| Solar panel capacity [kW] | 1 |
| Solar Azimuth [°] | 164.3853 |
| Solar Pitch [°] | 38.67047 |

363 The demand data used for this study was hourly measurements of electrical energy of 1157 households which was
 364 made available by Hildebrand Technology. Based on a confidentiality agreement, the data did not have any
 365

366 information with regard to the location of the households, and it was not possible to associate any meteorological
367 information to it. The period covered by the dataset was from the 1st June of 2013 until the 30th of May 2016 and
368 the electrical energy was measured in [Wmin]. The electricity demand data was clustered with a view to
369 extracting representative consumer patterns which were used as an input in the predictive data-driven methods.
370 Normalisation is particularly important for most machine-learning methods; as non-normalised data can result in
371 computationally ill-conditioned calculations. A representative example of this is with neural networks with a
372 sigmoid activation function, for which, if the values of t are large, the gradient of $f(t)$ will become very small.
373 This makes the training procedure unproductive and inefficient. The algorithm that was chosen for the
374 classification of the demand data was the K-Spectral Centroid, which is a partitioning method based on the k-
375 means approach that classifies data with regard to their shapes. The MATLAB code was available from the
376 Stanford Network Analysis Project (SNAP) [152].

377 **2.2. Forecasting Methods**

378 In forecasting a time series with a data-driven approach, there are three types of architecture that can be used,
379 namely the input-output approach (I-O), the non-linear autoregressive (NAR) and the nonlinear autoregressive
380 with exogenous inputs (NARX). The main difference between these architectures is the type of data each method
381 accepts as inputs. The former uses any kind of input except the past value of the target series. The second approach
382 uses only the past values of the target series, and finally the latter uses both the target's previous values as well as
383 exogenous inputs. It can be easily seen that the NARX procedure outperforms the former two when the exogenous
384 inputs are correlated to the targets, as it carries more information about the system. These three main types of
385 models are listed in the following.

$$386 \quad y(t+p) = f(x(t), x(t-1), \dots, x(t-d_x)) \quad (1)$$

$$387 \quad y(t+p) = f(y(t), y(t-1), \dots, y(t-d_y)) \quad (2)$$

$$388 \quad y(t+p) = f(x(t), x(t-1), \dots, x(t-d_x), y(t), y(t-1), \dots, y(t-d_y)) \quad (3)$$

389 where $y(t)$ is the output time series of the dependent variable that is predicted (in this case wind power output,
390 solar power output and electricity demand), $f(\cdot)$ represents the “black box” model used for prediction. $x(t)$ is
391 the input time series (independent variable). d_y and d_x are the feedback and input delays which correspond to
392 the number of past values of the target or the inputs, respectively, that are used for the prediction of the future
393 value. p represents the number of steps ahead for which the future behaviour is being predicted ($p \geq 1$).

394 The present research examines the performance of artificial neural networks (ANN), support vector regression
395 (SVR) and Gaussian process regression (GPR) for predicting power generation from wind and solar energy, as

396 well as the stochastic behaviour of electricity demand. These methods were chosen for various reasons that were
397 associated with either their proven good performance (ANN, SVR) or their potential to provide high accuracy
398 forecasts and black-box models in other applications (GPR).

399 **2.2.1. Artificial Neural Networks**

400 Artificial neural networks (ANNs) are developed in analogies with the architecture of the human brain, enabling
401 it to interpret a great amount of data and transform them into actionable knowledge [153]. A thorough survey of
402 literature suggests that for the prediction of time series, dynamical neural networks are most efficient as they can
403 be trained and tuned to predict time-dependent data. Amongst the various developments of dynamical neural
404 networks, the Non-linear AutoRegressive model with exogenous inputs (NARX) neural network has gained great
405 popularity in the research community [154–159].

406 In order to obtain a neural network that is both accurate and effective in terms of computational cost, there are
407 many parameters that are required to be tuned and many options that need to be selected. More specifically, prior
408 to training a NARX neural network, the two key parameters of the autoregressive model, namely the input (d_x)
409 and feedback (d_y) delays need to be determined as well as the number of neurons in the hidden layer. Upon
410 finding the optimal architecture, the next step is to find the appropriate training method. As will be seen in the
411 results section, a fully connected ANN with a single hidden layer would suffice for accurate modelling of power
412 generation from wind and solar energy, as well as electricity demand. While details comparison of various ANN
413 methods are beyond the scope of the present study, the research are generalizable in the sense that more complex
414 neural network architectures could also gain similar or better performance. The overall procedure that was
415 followed in the present research, in order to build the NARX models for every one of the three prediction studies
416 (wind, solar and demand forecasting) is depicted in **Figure 1**. It should be noted that in principle, the optimal
417 values of the input delays, the feedback delays and the number of neurons in the hidden layer are all interrelated.
418 However, simultaneous optimization of these structural parameters poses a formidable bi-level optimization
419 problem, as they are indeed hyper-parameters, and their values must be fixed before the training process could
420 start. Nevertheless, as will be shown in Results section, even under the simplifying assumption that they could be
421 optimized independently, excellent results can be achieved. The artificial neural networks were implemented
422 using the Neural Network Toolbox™, and the Optimization Toolbox™ (for the case of the genetic algorithm) in
423 MATLAB. The options for stochastic gradient descent (SGD) were activated in order to manage the computational
424 costs.

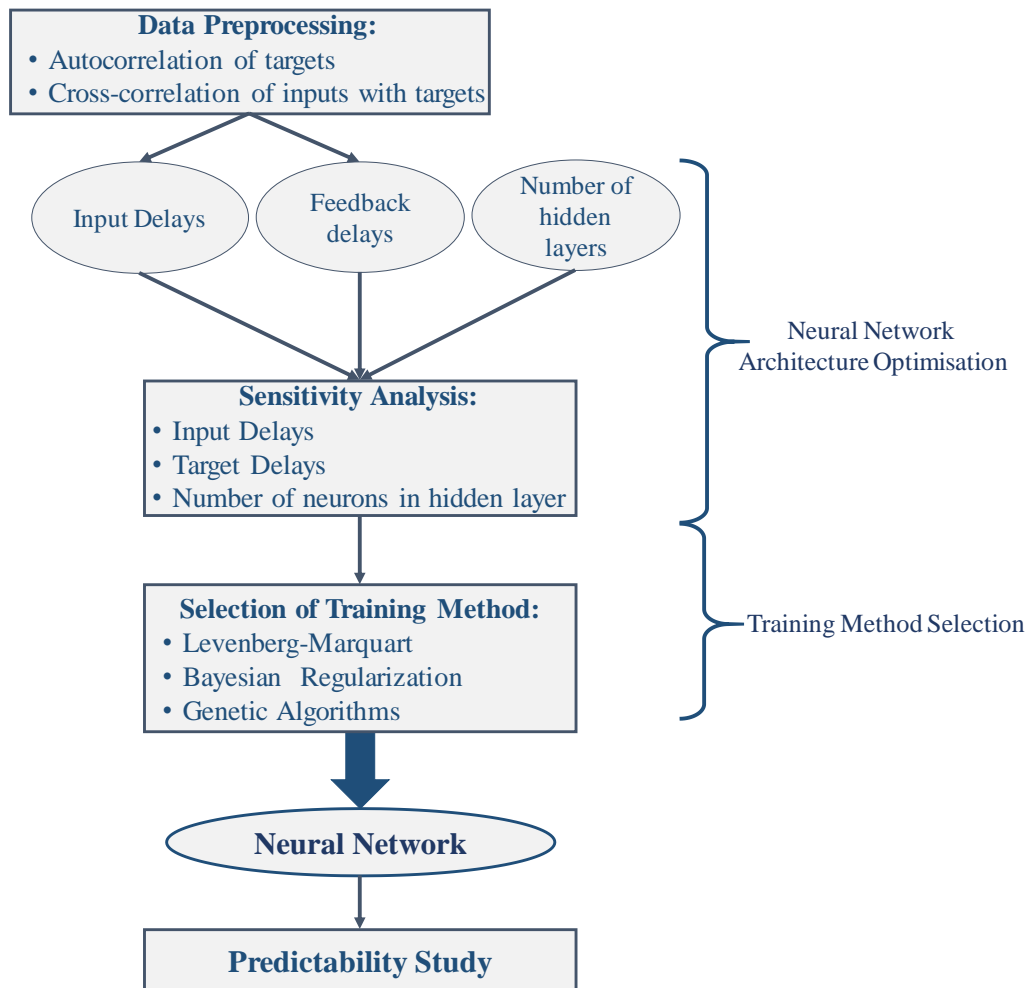


Figure 1. Framework for tuning NARX neural network parameters and selecting the training method

425

426

427

428

429

430

431

432

433

434

435

436

437

438

439

Neural networks are highly efficient in predicting empirical data. It is shown that for a sufficiently large number of neurones, even only one hidden layer suffices to simulate any nonlinear function from a compact input set [160–162]. Therefore, in order to minimize the training effort and without loss of generality, the neural networks designed in this research consisted of a single layer. Then the number of neurons in the hidden layer of the neural network were optimized until no further improvement was achieved. In order to set the input and feedback delays, a correlation analysis was performed on the data, and then through a trial and error procedure, the best performing delays were selected for each model [154,157]. It should be noted that artificial neural networks often suffer the two problems of overfitting and premature convergence to local solutions. In order to tackle these issues, the ANN model was first trained with a Genetic Algorithm (GA), and then its solution was applied as the initial guess for the Levenberg-Marquardt and Bayesian Regularization methods. The justification is that GA is a stochastic global optimization algorithm and is efficient in handling local solutions, while the role of the other two methods is to refine the solution. In order to handle the overfitting issues, prior to the training procedures, the available data was split into three subsets, namely the training set (typically 70%), the validation set (15%) and finally the testing set

440 (15%). The training algorithm uses the training set to update the weights and biases of the neural network by
441 minimising the mean squared error. At the same time, however, an additional mean squared error is calculated
442 which corresponds to the validation data. In the beginning of the training procedure, both of these errors drop, but
443 as the neural network becomes more and more tuned to the training data, the validation error will start increasing.
444 From the moment this happens, the training algorithm runs for a predetermined number of times. If by the time it
445 has ran for this number of steps, the validation error does not decrease, the training terminates and the weights
446 and biases that correspond to the lowest validation error (that occurred during those iterations) are returned. The
447 testing data is utilised after the training is completed, in order to examine the network's performance. This
448 procedure is referred to as early stopping, since the training algorithm terminates prior to reaching the optimal
449 point [163].

450 **2.2.2. Support Vector Regression (SVR)**

451 Support vector machines are a renowned classification algorithm, which categorise data accurately, do not have
452 any difficulty with the number of dimensions of data and require only a small training sample, but they are
453 computationally demanding if caution is not taken [164]. By applying minor alterations this method can be also
454 implemented for regression purposes [165,166]. Support Vector Machines and ϵ -SVR are applicable to static
455 problems, and therefore, the black box models that can be built through this method can only be used for
456 simulation. In order to make step-ahead predictions further modifications need to be made, in order to build a
457 NARX architecture for the SVR that could give a dynamic effect to the model. In the present research, a toolbox
458 developed in KU Leuven was employed, which is based on the Least Squared Support Vector Regression (LS-
459 SVR) methodology, and allows the development of a dynamical model [167,168].

460 **2.2.3. Gaussian Process Regression (GPR)**

461 Gaussian Process Regression (GPR) is a non-parametric probabilistic kernel model. This machine-learning
462 method has gained more and more ground in the literature over the past few years [169]. This method not only
463 can be applied for prediction, but also can provide the confidence interval for each point in the prediction which
464 quantifies the uncertainty of the forecast. Essentially, a Gaussian process is generalisation of the respective
465 probability distribution. The Gaussian distribution takes an input vector and computes its probability whose
466 characteristics are a mean and variance. The probability of an input time series vector, for each time step, is
467 computed. Therefore instead of having a mean and variance that are scalars, the GPR model calculates a mean
468 and covariance vector [169–171]. It should be mentioned that the GPR, similarly to SVR, cannot dynamically
469 predict ahead as it is not a dynamic algorithm. For this purpose, a toolbox developed by Stepančić and Kocijan

470 [172] was applied in this study that can build a NARX architecture and allows predictions to be made for any time
 471 horizon.

472 3. Results and discussion

473 This section presents the results. It is divided into four sections which correspond to the three different types of
 474 predictions that were conducted, namely wind power, solar power, and electricity demand forecasting, followed
 475 by the last section in which a comparison of the different models and datasets is made. For each type of prediction,
 476 the structure of the results begins with firstly demonstrating the various features of the data and follows with
 477 evaluating the performance of the various predictive analytics methods. The various inputs used for each case of
 478 wind power, solar power, and electricity consumption forecasting are given in **Table 6**. It should be mentioned
 479 that throughout this paper a prediction time step is equivalent to an hour. Moreover, the term “model” is used to
 480 denote the black box model that is fed by the inputs of the present time and predicts the response of the system at
 481 the present time, meaning that no forecasting takes place.

482 **Table 6.** Inputs used for wind power, solar power, and electricity demand forecasting.

| Input Vectors | Wind Power Prediction | Solar Power Prediction | Electricity Demand Prediction |
|-------------------------------------|-----------------------|------------------------|-------------------------------|
| Hourly Variable | ✓ | ✓ | ✓ |
| Seasonal Variable | ✓ | ✓ | ✓ |
| Wind Power (KW) | ✓ | | |
| Solar Power (KW) | | ✓ | |
| Electricity Energy [Wmin] | | | ✓ |
| Temperature (°C) | ✓ | ✓ | |
| Wind Speed at 10m ($\frac{m}{s}$) | ✓ | | |
| Direct irradiance (KW) | | ✓ | |
| Diffuse irradiance (KW) | | ✓ | |

483

484 3.1. Wind power forecast

485 3.1.1. Data pre-processing

486 In **Table 7** the maximum absolute value for each cross-correlation is given, in order to quantify the dependence
 487 of wind power with regard to each input. It can be seen that wind power is directly dependent on wind speed
 488 (**Figure 2b**), whereas the correlation with hourly (time) variable is weak (**Figure 2e**). This is expected since wind
 489 speed is the driving force of the turbines, and even though wind is a result of the temperature gradients caused by
 490 solar irradiance, the time of the day seems to have an indirect and random interrelationship with power. However,
 491 it can be seen that the time of the year (**Figure 2d**) as well as the temperature (**Figure 2c**) influence the wind
 492 power.

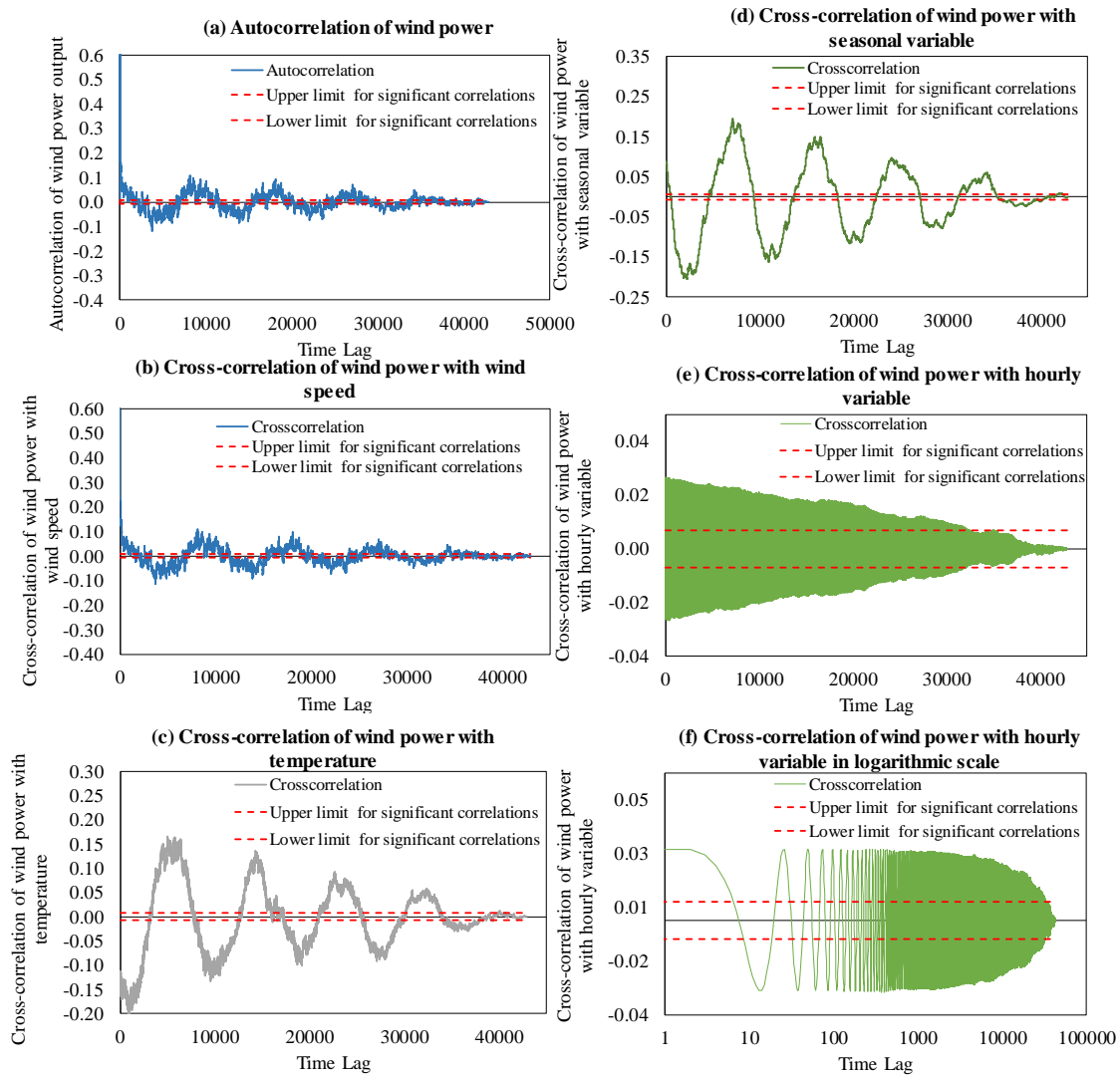
493

Table 7. Maximum absolute cross-correlations for input data used for wind power prediction

| Input | Maximum absolute correlation |
|-------------------|------------------------------|
| Hourly variable | -0.026563 |
| Seasonal variable | -0.205345 |
| Wind Speed | 0.979487 |
| Temperature | -0.206958 |

494

495



496

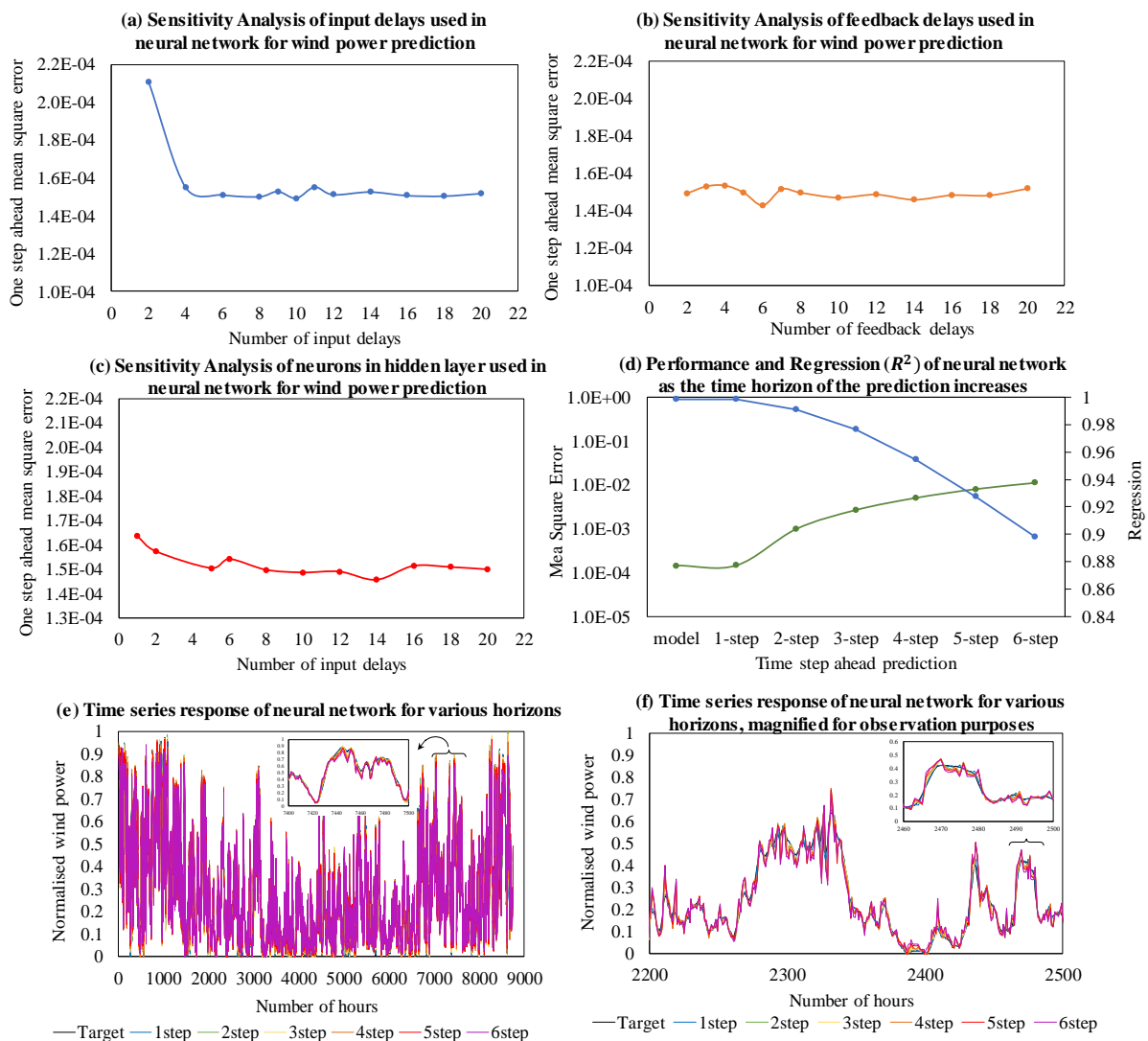
497

Figure 2. Cross-correlations for input data applied for the wind power prediction

3.1.2. Forecasting wind power with Artificial Neural Networks (ANN)

499 For the implementation of neural networks, firstly a sensitivity analysis was conducted with which the delays of
 500 the network as well as the number of hidden neurons were determined. Moreover, the response of the selected
 501 neural network was tested for a number of different time horizons. In order to select the most fitting value for each
 502 instance, two factors were taken into consideration. Firstly, the mean square error (MSE) of the neural network's

503 response with regard to the testing data for the one-hour ahead prediction was taken into consideration, which is
 504 depicted in the vertical axis of **Figures 3a-c**. Secondly, the error's autocorrelation and cross-correlation with each
 505 input were calculated as graphically presented in **Figures 2d-f** for each simulation, and the simulation for which
 506 the most of the correlations that were within limits was selected. In particular, especially for the neural networks
 507 whose response did not significantly change, the second factor was utilised to make a selection.
 508 **Figures 3a-c** show that there is a point beyond which the performance of the neural network did not significantly
 509 change, as the input delays, the feedback delays and the number of neurons in the hidden layer increased.
 510 Therefore, the aforementioned second factor was taken into consideration and the characteristics of the neural
 511 network that were chosen were 10 input delays, 12 feedback delays and 10 neurons within the hidden layer.



512

513

Figure 3. The sensitivity analysis and performance of ANN for wind power prediction

514 With regard to the predictability analysis, different neural networks were developed for each time horizon. The
 515 accuracy as well as the regression values of these neural networks are given in **Table 8**, and are represented in
 516 **Figure 3.d**.

517 **Table 8.** Regression and MSE values for various time horizons regarding wind power prediction with neural networks

| Time horizon | Regression (R ²) | Mean Square Error |
|--------------|------------------------------|-------------------|
| model | 0.99874 | 1.4473E-04 |
| 1-step | 0.99874 | 1.4560E-04 |
| 2-step | 0.9914 | 9.9105E-04 |
| 3-step | 0.97675 | 2.7000E-03 |
| 4-step | 0.95477 | 5.1000E-03 |
| 5-step | 0.92761 | 0.0081 |
| 6-step | 0.89807 | 0.0113 |

518
 519 As expected, the accuracy and the fitting capability of the model drops as the time horizon of the prediction
 520 increases, since the model is given no knowledge for the interval between the current state and the time horizon
 521 of the prediction. This can also be observed in **Figure 3.e and f**, where the response of the neural network is given
 522 for all the predicted time horizons that were tested. The cooler colours denote the shorter time horizons and it can
 523 be observed that they are closer to the target series (black line). It seems that the neural network's response
 524 becomes less smooth as we move along to longer prediction steps.

525 The forecasting error of the ANN model for predicting the wind power generation is reported in the second column
 526 of **Table 9**.

527 **Table 9.** The performance of ANN training algorithms for wind power generation, solar power generation and
 528 electricity demand

| | Training error for wind power prediction | Training error for solar power prediction | Training error for electricity demand |
|-------------------------|--|---|---------------------------------------|
| Levenberg-Marquardt | 0.000147 | 0.00032439 | 0.000846 |
| Bayesian Regularization | 0.00014342 | 0.00026489 | 0.000747 |
| Genetic Algorithm | 0.0108 | 0.0252 | 0.0364 |

529
 530
 531

532 **3.1.4. Forecasting wind power with Support Vector Regression**

533 As the SVR machine-learning method is stationary, it cannot be directly implemented to a time series problem
534 that will be built to forecast. For this reason, a different toolbox from the default respective one in MATLAB (ϵ -
535 SVR) was utilised that could use a NARX architecture in conjunction with LS-SVR for time series forecasting.
536 The sensitivity analysis that took place for tuning the SVR was done for the MATLAB toolbox (ϵ -SVR) in which
537 the three available kernel functions were tried, namely the linear, the polynomial and the radial basis function
538 (RBF). Upon testing the various available kernels, it was found that the RBF was more suited for this case.

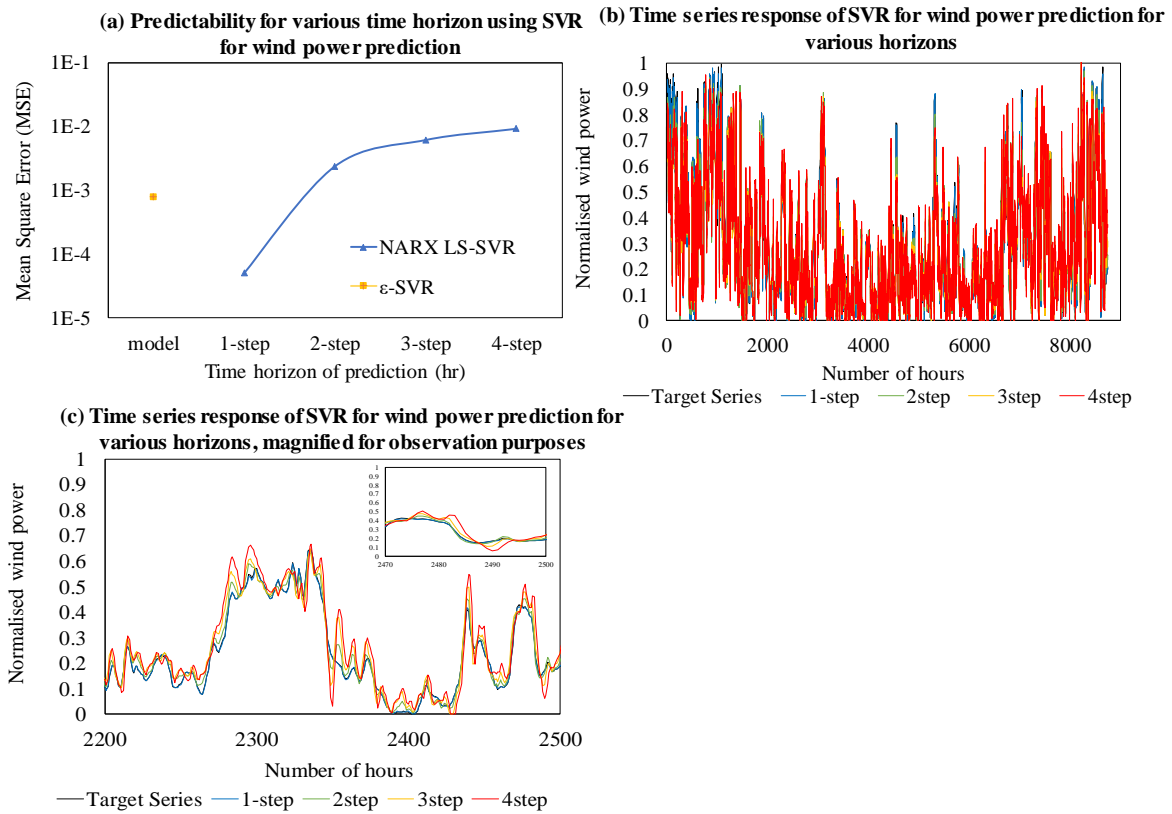
539 **Table 9.** MSE values for various time horizons regarding wind power prediction with SVR

| Time horizon | Mean Square Error (Testing) |
|--------------------------|------------------------------------|
| Model (ϵ -SVR) | 0.000797 |
| 1-step (NARX LS-SVR) | 0.0000503 |
| 2-step (NARX LS-SVR) | 0.0024 |
| 3-step (NARX LS-SVR) | 0.0062 |
| 4-step (NARX LS-SVR) | 0.0093 |

540

541 In **Table 9**, the performance indicator is given for all the time horizons for which predictions were conducted. As
542 mentioned earlier, the Model (ϵ -SVR) is stationary, i.e., with an input at a given time provides the response of the
543 system for the same time. As can be seen in **Figure 4.a**, the Model (ϵ -SVR) has a much greater error than when
544 the LS-SVR predicts one hour ahead. This observation should be attributed to the fact that the ϵ -SVR does not
545 have an autoregressive architecture, which means that to make a prediction this method uses only the input that is
546 specific to that particular time, and does not use the past values of the target series at all. The time-series responses
547 for each time horizon are given in **Figure 4.b**, and magnified in **Figure 4.c**, for various time steps. Similar to the
548 neural networks, as the time horizon of the prediction increases, the accuracy of the model decreases.

549



550

551

Figure 4. The sensitivity analysis and performance of the SVR for wind power prediction

552 3.1.4. Forecasting wind power with Gaussian Regression Process

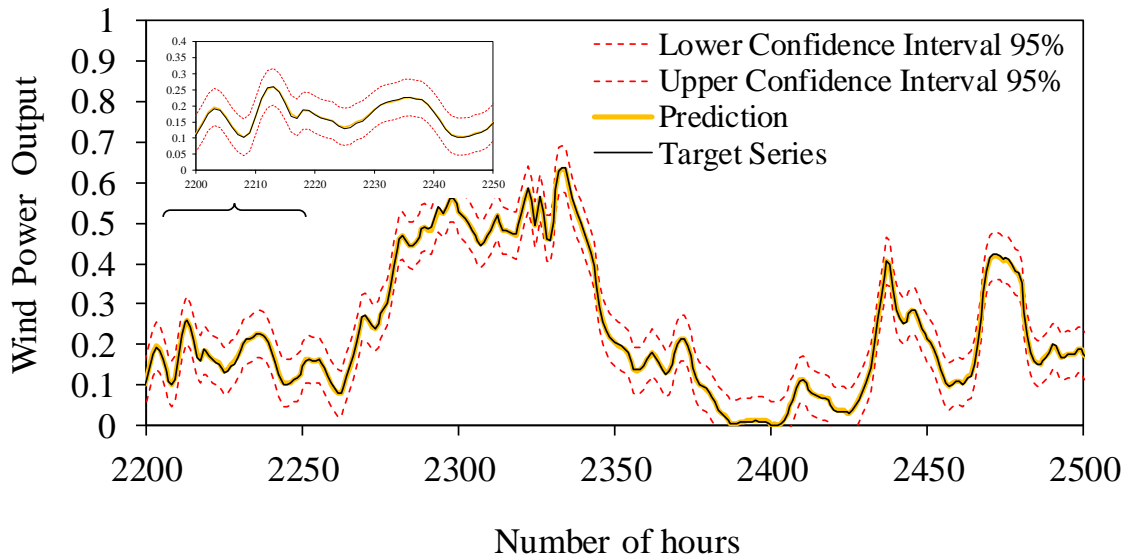
553 The sensitivity analysis conducted for the GPR included the establishment of the best kernel function that could
 554 be used to predict the response of the wind power as it was given an input vector that included the hourly variable,
 555 the seasonal variable, the wind speed and the temperature. The kernels that were tested are the ones listed as well
 556 as the performance of the model for each one of the cases is listed in **Table 10**. The best testing performance was
 557 provided by the kernel Matern 32, although the best training performance was given from ARD Matern 32. It can
 558 be observed that there is a trend in the listed performances which signifies that the ARD kernels give a good
 559 training performance but their testing performance is degraded, whereas the others have the opposite effect except
 560 for the squared exponential that seems to have a similar training and testing performance. Since it is sought to
 561 have good generalisation in the designed models, the testing performance is prioritised and therefore for wind
 562 power prediction the kernel Matern 32 was selected. Finally, in **Figure 5** the response of the GPR model for wind
 563 power prediction is represented and it can be noticed that overall the GPR captures the data very well and the
 564 target series lies always within the confidence intervals. Furthermore, it seems that there is more uncertainty
 565 associated with the time the wind power reaches local maxima and minima.

566

Table 10. Training and Testing Performance of GPR for various kernel functions for wind power prediction

| Kernel function | Training Performance (MSE) | Testing Performance (MSE) |
|-------------------------|----------------------------|---------------------------|
| Squared exponential | 8.0220E-04 | 8.2141E-04 |
| Matern 32 | 8.2351E-04 | 7.5198E-04 |
| Matern 52 | 8.0885E-04 | 7.9520E-04 |
| ARD Squared Exponential | 7.8194E-04 | 8.4339E-04 |
| ARD Matern 32 | 7.8154E-04 | 8.4127E-04 |
| ARD Matern 52 | 7.8162E-04 | 8.4274E-04 |

567



568

Figure 5. Time series response of GPR for wind power prediction (present time) magnified for observation purposes

569

570

571

3.2. Solar power forecast

572

3.2.1. Data pre-processing

573

The methodology and the steps required for solar power prediction are identical to the respective ones conducted for wind power prediction. This is due to the fact that the data were acquired from the same source, and therefore the same pre-processing steps were needed. However, due to the discontinuous nature of solar power, the results gained from this dataset were quite different.

577

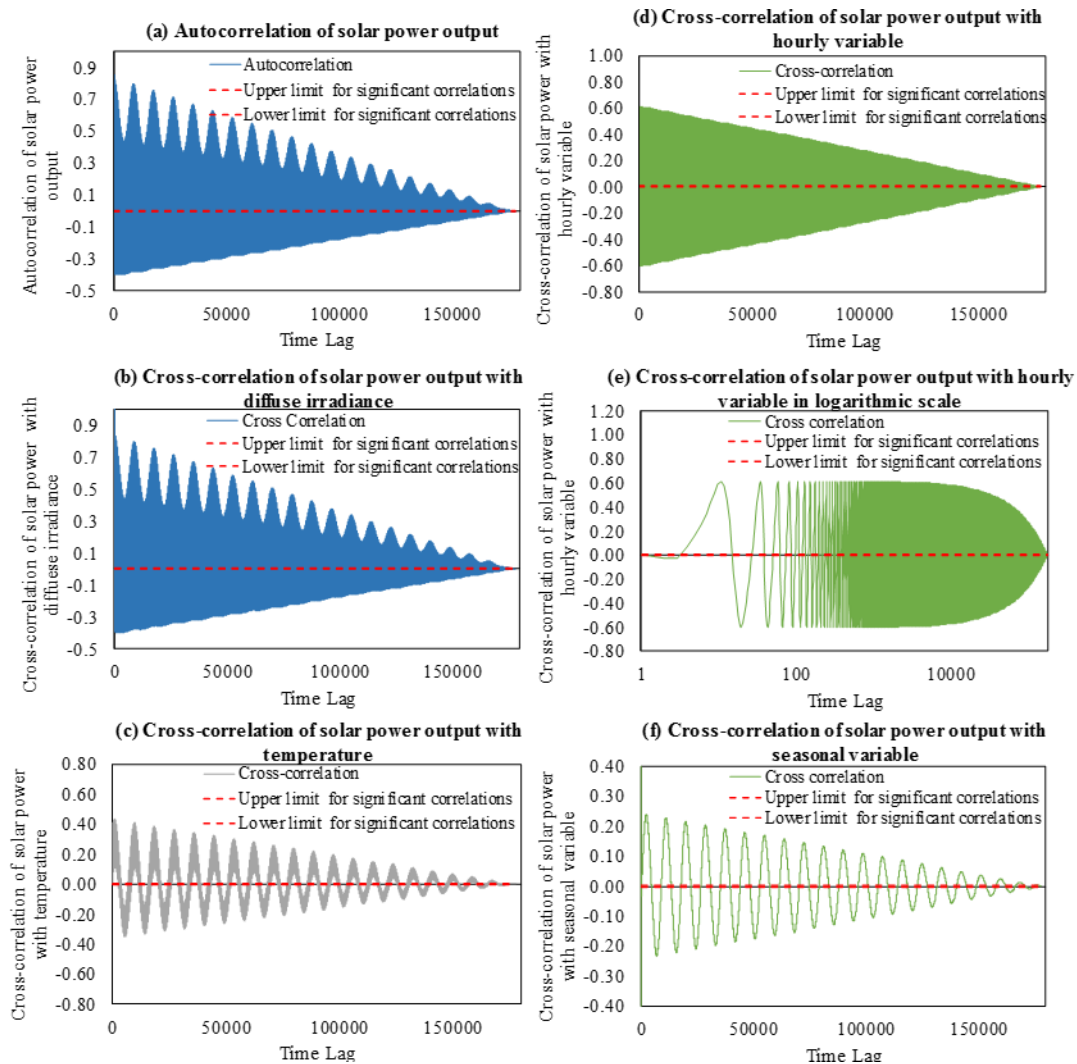
In **Table 11** the maximum absolute cross-correlations of the solar power with each respective input are given. It should be noted that the reason the autocorrelation is not included in this table is that its maximum value is always 1 and corresponds to the zero-time lag (**Figure 6.a**). Equivalently to wind power, the two variables that seem to be related more closely to the solar power output are the direct and diffuse irradiance (**Figure 6.b**). The temporal variables and temperature have an entirely different relation, though. The time of the day has a greater effect on the solar power output than the time of the year, which is expected as the photovoltaics have a discontinuous response; they produce energy during daylight only (**Figures 6.c-f**).

584

Table 11. Maximum absolute cross-correlations for input data used for solar power prediction

| Input | Maximum absolute correlation |
|--------------------|------------------------------|
| Hourly variable | 0.612193 |
| Seasonal variable | 0.241428 |
| Direct Irradiance | 0.963682 |
| Diffuse Irradiance | 0.812037 |
| Temperature | 0.432654 |

585
586



587

588

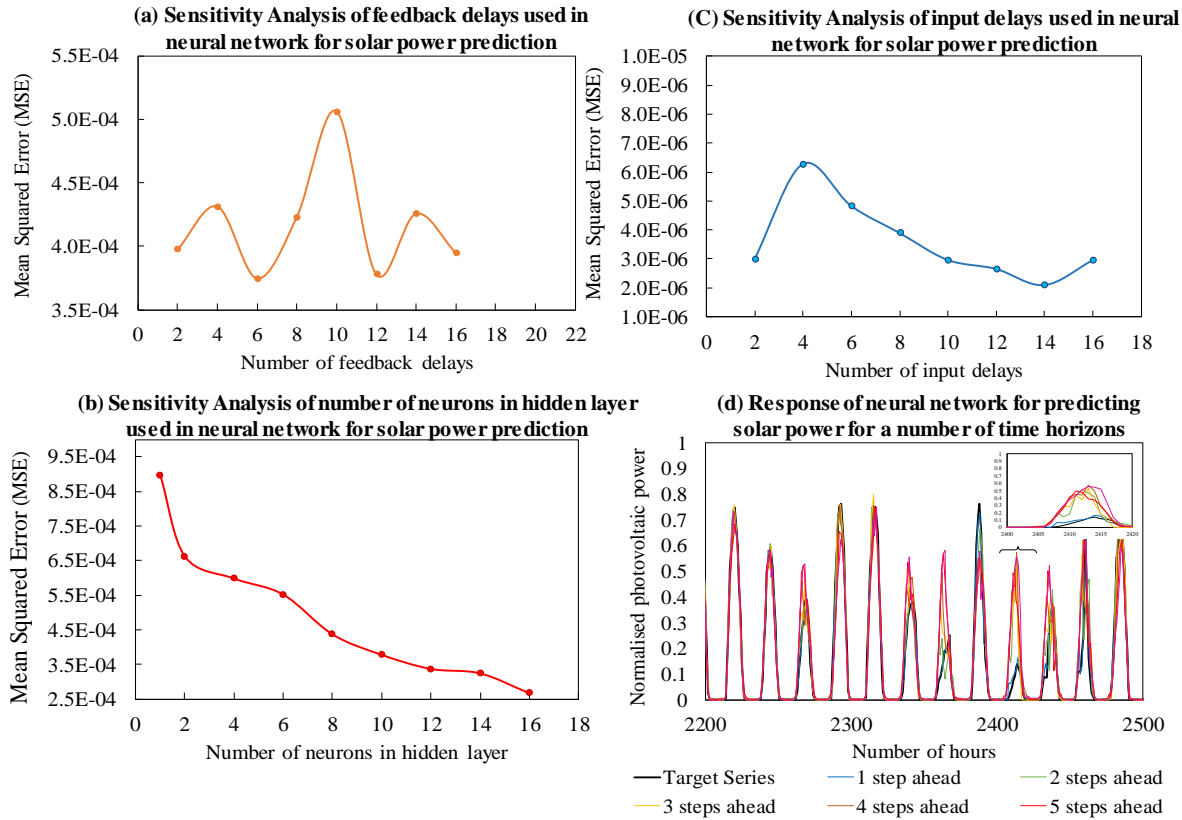
Figure 6. Cross-correlations for input data applied for the solar power prediction

589

590 3.2.2. Forecasting solar power with Artificial Neural Networks

591 The framework in **Figure 1** was followed to establish the ANN's architecture. More specifically, the feedback
592 delays (**Figure 7.a**) were first studied, followed by the input delays (**Figure 7.b**), and the number of neurons
593 within the hidden layer (**Figure 7.c**). By allowing these parameters to take various values a nonlinear response
594 can be observed, which is distinctively different from respective sensitivity analyses conducted for the case of

595 wind power. In addition, it should be mentioned that even though in **Figure 7.c** it seems that if the number of
 596 neurons was increased, the accuracy of the ANN could further improve, this was not pursued since the model
 597 became very computationally expensive when the number of hidden neurons took a value over 14. The parameters
 598 that were selected for the neural network's architecture were 12 input delays, 12 feedback delays and 14 neurons
 599 within the hidden layer.



600

601

Figure 7. The sensitivity analysis and performance of ANN for solar power prediction

602

603

604

605

606

607

608

609

610

611

With a view to generating predictions for various future time horizons, six different NARX neural networks were constructed. The performance of each of these networks is listed in **Table 12**. It can easily be identified that the accuracy of the neural network decreases as the time horizon increases. This trend can be observed additionally from the response of the neural networks for the various time horizons which is visualized in **Figure 7.d**. The one-hour ahead closely follows the target series and shows a very good performance, followed by the two-hour ahead prediction, which although in general, it captures the target series well, there are some instances for which it did not converge to the desired value. From 3 hours and further, although for some days a satisfactory accuracy is achieved, there are numerous instances for which the predictions show a 200% error of solar power production which can be problematic if these models are used in an actual practice. **The forecasting error of the ANN model for predicting the solar power generation is reported in the third column of Table 9.**

612

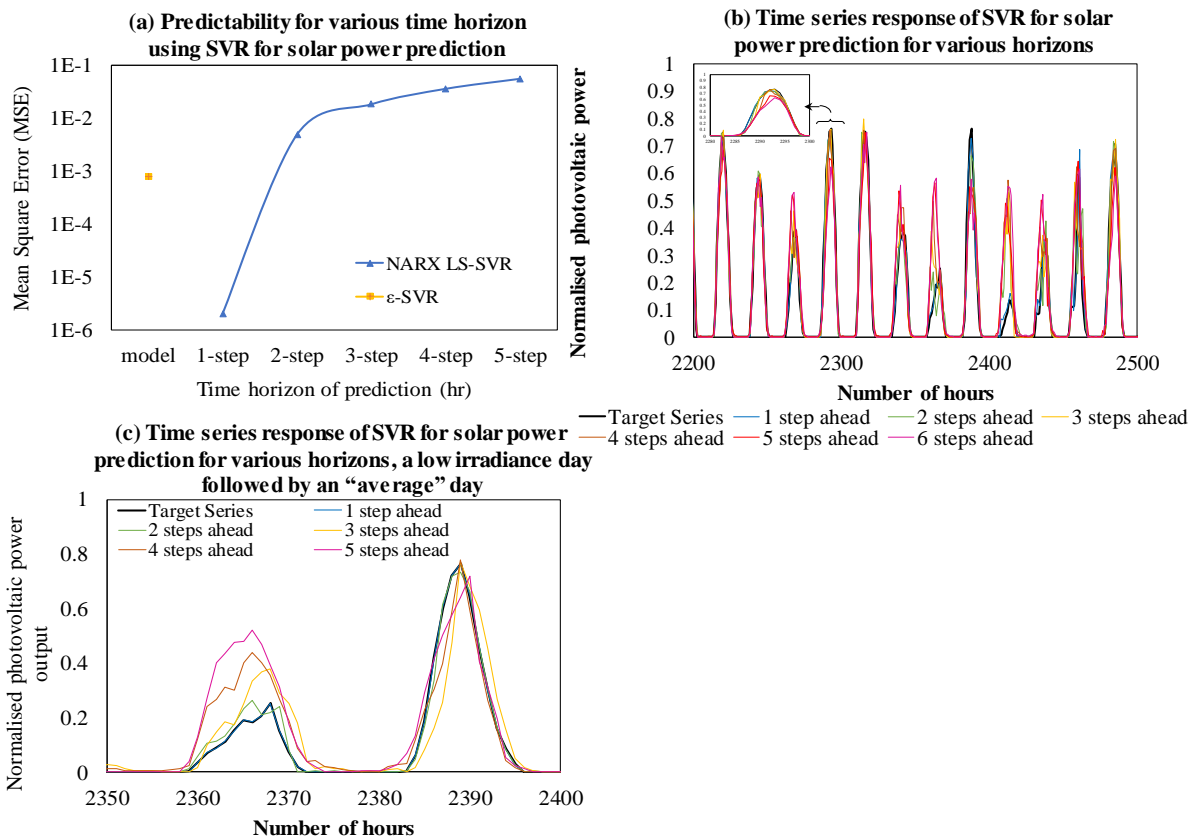
Table 12. MSE values for various time horizons regarding solar power prediction with neural networks

| Time horizon | Mean Square Error |
|--------------|-------------------|
| model | 0.00031467 |
| 1-step | 0.00032632 |
| 2-step | 0.0028 |
| 3-step | 0.0037 |
| 4-step | 0.0047 |
| 5-step | 0.0061 |
| 6-step | 0.0065 |

613

614 **3.2.3. Forecasting solar power with Support Vector Regression**

615 Similar to the case of wind data, a sensitivity analysis in the MATLAB toolbox (ϵ -SVR) was conducted in order
 616 to establish the most fitting kernel function out of the choices of linear, polynomial and radial basis function
 617 (RBF). The polynomial kernel did not converge and did not manage to capture the underlying pattern of the solar
 618 dataset. The linear kernel provided an error of 0.0114 but did not terminate due to reaching the maximum number
 619 of iterations and finally, the RBF which was deemed to be most suitable, converged with the performance of
 620 0.0015.



621

622

Figure 8. The sensitivity analysis and performance of SVR for solar power prediction

623 The solar power was forecasted for a number of time horizons with the NARX LS-SVR method by applying the
624 RBF kernel and setting the delays for the input vector and the target to 12. The performances for each
625 corresponding time horizon is given in **Table 13**, and depicted in **Figure 8.a**, where it can be seen that for one
626 step ahead prediction a significant accuracy is accomplished. The reason for this is that the model that predicts
627 the present response has a greater error is identical to the respective one given for wind power, that is to say, the
628 ϵ -SVR does not have an autoregressive architecture. In **Figure 8.b**, the response of the time series for all the time
629 horizons simulated are provided and similarly to the case of wind, as it moves towards larger prediction horizons,
630 the model tends to lose its accuracy. One striking observation, though is that the accuracy does not seem to drop
631 for all time steps equivalently, as in the case of wind, but mostly for the days for which a small amount of solar
632 power is produced (**Figure 8.c**). The reason behind this phenomenon is in contrast to the wind power case, the
633 solar power is discontinuous. Therefore when the model is asked to predict 5 hours ahead at dawn it has no
634 knowledge of whether the solar irradiance will be limited throughout the day. This leads to the model giving a
635 prediction that has an average pattern over all the training data. On the other hand, when performing one-hour
636 ahead predictions the model can adjust its response if the day is cloudy, as it receives all the respective information
637 with only one hour delay. This is the reason for which when moving from the one step ahead prediction towards
638 longer time horizons, the error increases by approximately the power of 3.

639 **Table 13.** MSE values for various time horizons regarding solar power prediction with SVR

| Time horizon | Mean Square Error (Testing) |
|--------------------------|-----------------------------|
| Model (ϵ -SVR) | 0.0015 |
| 1-step (NARX LS-SVR) | 0.000002025 |
| 2-step (NARX LS-SVR) | 0.0049 |
| 3-step (NARX LS-SVR) | 0.0182 |
| 4-step (NARX LS-SVR) | 0.0356 |
| 5-step (NARX LS-SVR) | 0.0551 |

640

641 **3.2.4. Forecasting solar power with Gaussian Regression Process (GPR)**

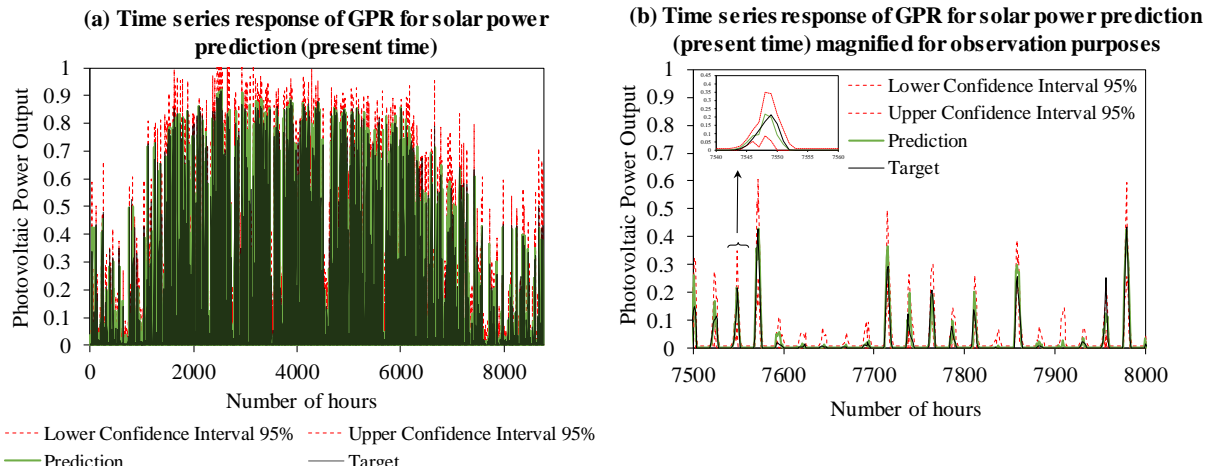
642 In order to tune the GPR for the prediction of solar power, a sensitivity analysis was conducted in order to establish
643 the best kernel function. From **Table 14** it can be seen that the Matern 52 kernel outperformed all others, and this
644 function was therefore selected to build the final GPR model. The response of the built model is depicted in **Figure**
645 **9.a** for all the testing data (the year 2014), and in **Figure 9.b** a total of 500 hours, with a view to providing a higher
646 resolution. Even though there are some instances where the prediction is not exactly fitted to the target series (as
647 was mostly for the case of the wind), the model gives satisfactory results and the target series for almost the
648 entirety of the time steps lies within the confidence intervals.

649

Table 14. Sensitivity analysis for appropriate kernel function selection for solar power prediction

| Kernel function | Training Performance | Testing Performance |
|-------------------------|----------------------|---------------------|
| Squared exponential | 1.5598E-05 | 3.3E-03 |
| Matern 32 | 9.2948E-06 | 3.2E-03 |
| Matern 52 | 6.4625E-06 | 1.9E-03 |
| ARD Squared Exponential | 7.9675E-06 | 2.2E-03 |
| ARD Matern 32 | 1.2948E-05 | 3.5E-03 |
| ARD Matern 52 | 8.7765E-06 | 2.1E-03 |

650



651

652

653

654

Figure 9. (a) Time series response of GPR for solar power prediction (present time) and (b) Time series response of GPR for solar power prediction (present time) magnified for observation

655

3.3. Electricity demand forecast

656

3.3.1. Data Pre-processing

657

3.3.1.1. Time Series Data Clustering

658

The case of electricity demand prediction was quite different from the respective wind and solar power for several

659

reasons. Firstly, owing to the fact that the dataset provided was in a disaggregated form and included the hourly

660

electricity consumption of 1157 households located around the world, the dataset required clustering. Secondly,

661

this data had no other inputs associated with it, due to privacy considerations. Finally, as this dataset was received

662

from actual measurement units that were installed in the households there are additional errors and uncertainties

663

affiliated with the data, such as instrument failures.

664

In order to perform the data clustering, the K-Spectral Centroid analysis was performed, which is a data clustering

665

technique that categorises time series data according to their shape [152]. As this is a partitioning data technique

666

the number of clusters needed to be set prior to executing the algorithm. In this study, the number of clusters for

667

which this algorithm was run are $K = \{2,3,4,5,6,7,8,10\}$. Beyond 10 clusters the households were thought to be

668

poorly split as there were only 610 households to be divided and some of the clusters were comprised of very few

669

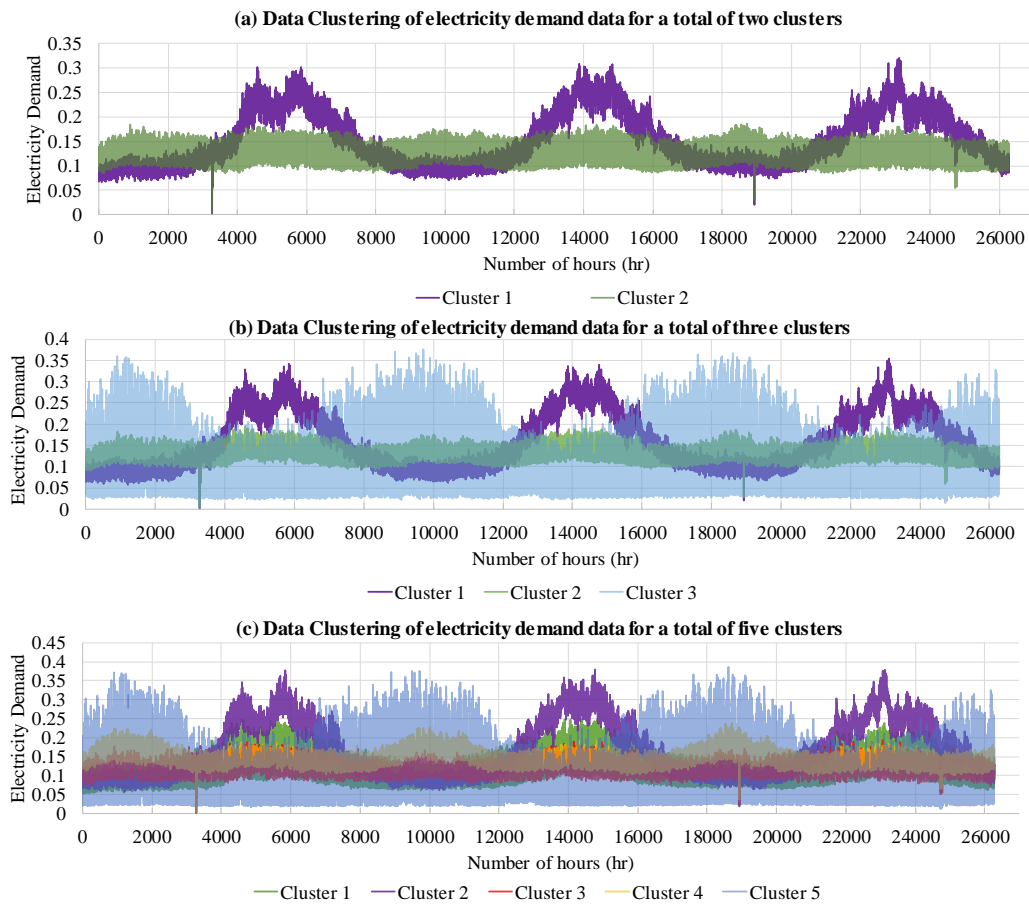
households.

670 In **Table 15** the numbers of houses that correspond to each cluster for each value of K are given. It can be seen
671 that overall for all cases, each cluster has a sufficient amount of information. In **Figures 10.a-c**, the division of
672 the data can be observed for different numbers of clusters for k=2,3,5. Over the various clusters, for all cases,
673 there is at least one of the patterns that has a distinctly different behaviour compared to the rest, as it seems to be
674 shifted by 6 months. These patterns that seem to have a six-month lag correspond to households in the southern
675 hemisphere since during the warmer months of the southern hemisphere, the northern hemisphere experiences
676 colder temperatures and vice versa. This observation stands due to the positive correlation between the electricity
677 consumption and the temperature.

678 **Table 15.** Number of households that correspond to each cluster, for each simulation

| Total number of clusters | 2 | 3 | 4 | 5 | 6 | 7 | 8 | 10 |
|--------------------------|-----|-----|-----|-----|-----|-----|-----|-----|
| cluster 1 | 220 | 166 | 240 | 164 | 225 | 164 | 124 | 95 |
| cluster 2 | 390 | 407 | 144 | 125 | 105 | 97 | 76 | 46 |
| cluster 3 | | 37 | 192 | 120 | 60 | 51 | 36 | 96 |
| cluster 4 | | | 34 | 167 | 104 | 111 | 57 | 31 |
| cluster 5 | | | | 34 | 84 | 94 | 88 | 90 |
| cluster 6 | | | | | 32 | 66 | 116 | 58 |
| cluster 7 | | | | | | 27 | 81 | 90 |
| cluster 8 | | | | | | | 32 | 48 |
| cluster 9 | | | | | | | | 26 |
| cluster 10 | | | | | | | | 30 |
| Total: | 610 | 610 | 610 | 610 | 610 | 610 | 610 | 610 |

679
680



681

682 **Figure 10.** Data Clustering of electricity demand data for the total of (a) two (b) three, and (c) five clusters.

683 The number of clusters that was selected was five which is graphically represented in **Figure 10.c**. The reasoning
 684 behind this decision is:

- 685 • The wind and solar data that correspond to a specific location in the UK and therefore the selected
 686 electricity demand pattern should at least correspond to the northern hemisphere
- 687 • The majority of households in the dataset are located in the northern hemisphere

688 As can be observed from **Figure 10.c** there are two distinct patterns that correspond to the northern hemisphere;
 689 Pattern 1 and Pattern 2. Finally, Pattern 1 was chosen because a larger number of households were within that
 690 specific cluster and also its pattern seems to be closer to what is expected from a household. Pattern 2 maintains
 691 large values throughout the winter there are some instances where little variation is observed, whereas Pattern 1
 692 seems to have a daily pattern in conjunction with a seasonal variation.

693 3.3.1.2. Data Autocorrelations

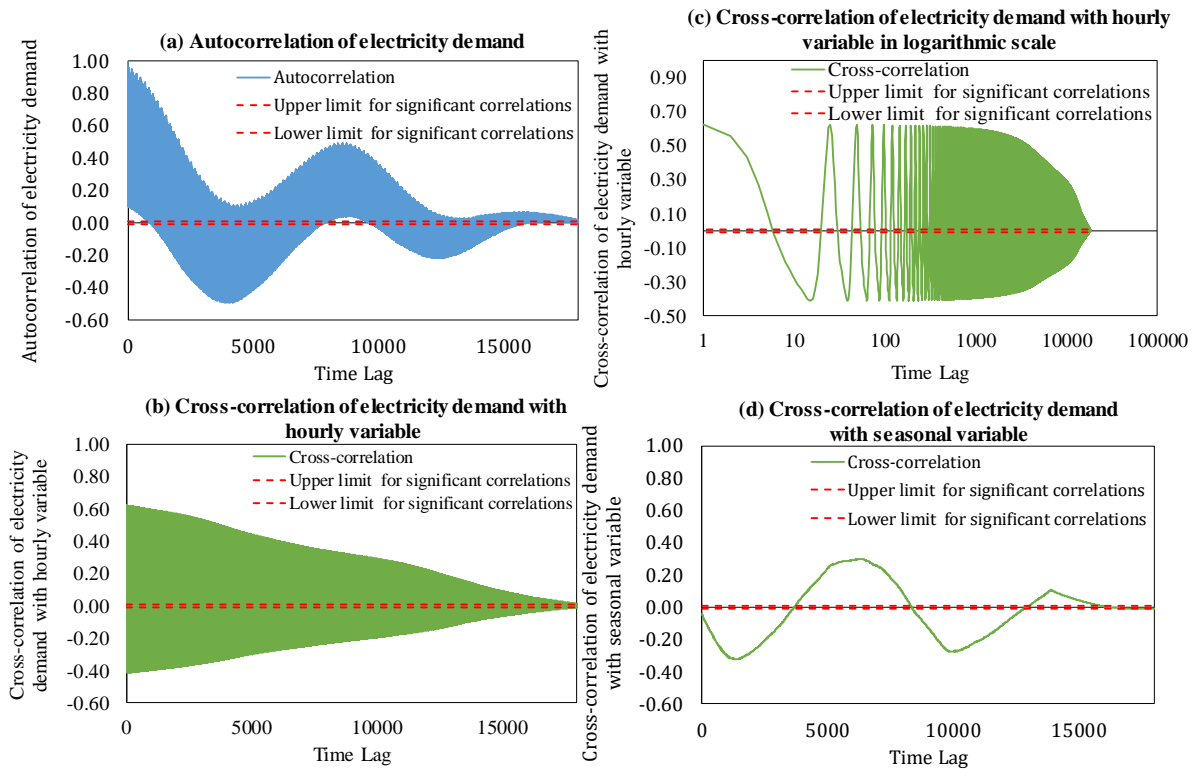
694 For electricity demand prediction although no other data was associated with it, for the predictive analytics two
 695 inputs were included, specifically the hourly and seasonal variables. By introducing these variables, it was hoped
 696 that the training of the models would be facilitated. This statement has proven to stand, as from **Table 16** it can

697 be observed that the maximum cross-correlations of each of the inputs can be considered to be significant,
 698 especially for the hourly variable.

699 **Table 16.** Maximum absolute cross-correlations for input data used for electricity demand prediction

| Input | Maximum absolute correlation |
|-------------------|------------------------------|
| Hourly variable | 0.622855 |
| Seasonal variable | 0.29743 |

700 Similar to the case of solar power, the autocorrelation of demand shows both a yearly and daily repetition and the
 701 values do not decrease as steeply as for the case of wind power (**Figure 11.a**). The dependence of the demand on
 702 the time of the day and year is represented in the cross-correlation graphs depicted in **Figure 11.a-c**. A noteworthy
 703 characteristic of all the graphs in this section is that they are not entirely symmetrical as opposed to the wind and
 704 solar data. This is due to the fact that this dataset is a result of actual measurements and therefore has the
 705 stochasticity associated with them.



706

707

Figure 11. Cross-correlations for input data applied for the solar power prediction

708

3.3.2. Forecasting electricity demand with Artificial Neural Networks

709

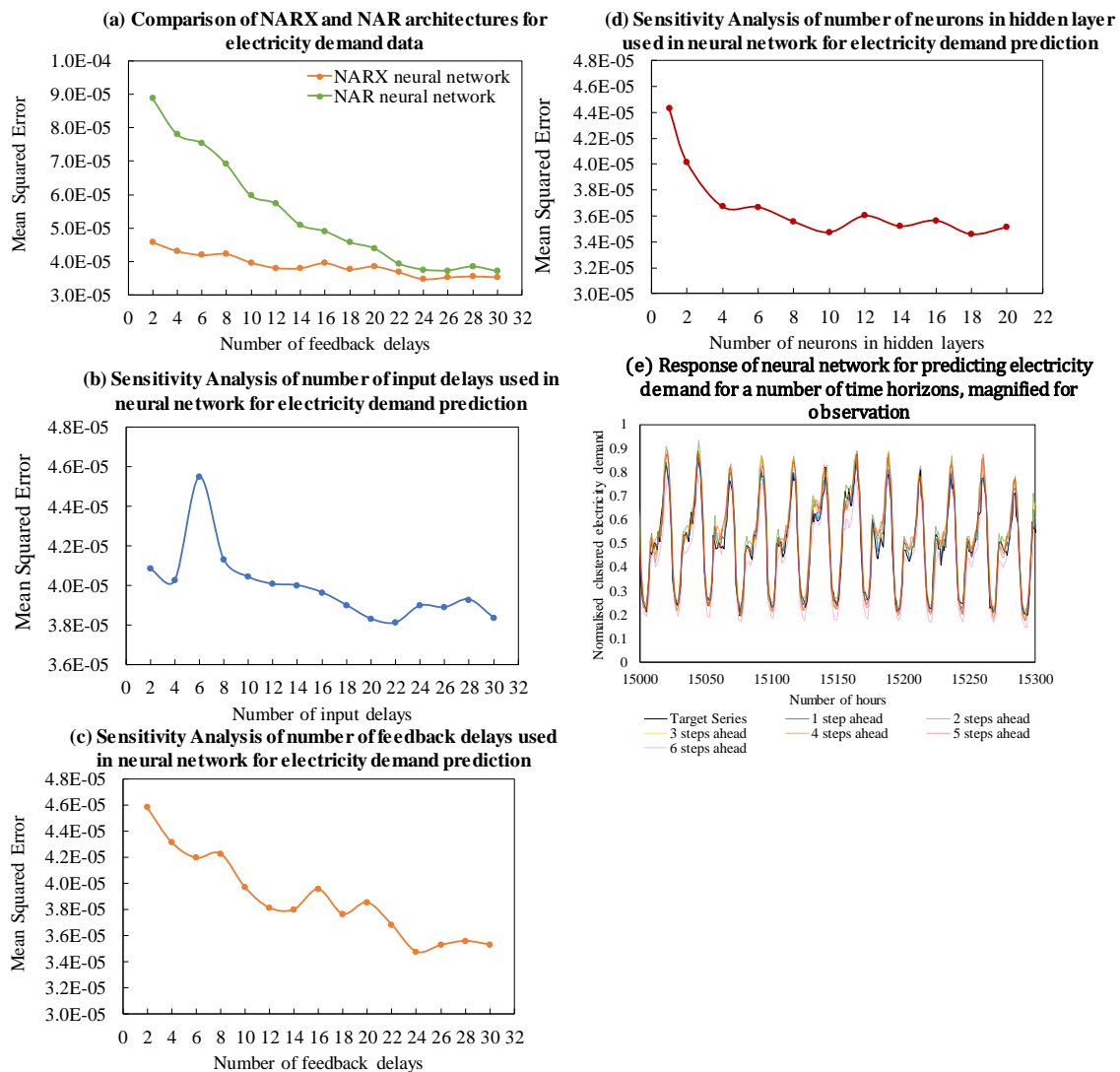
710

711

712

As mentioned earlier, the demand data had no inputs associated with it, but during the pre-processing procedure, the hourly and seasonal variables were introduced to the electricity demand dataset with an aim to facilitate each of the predictive analytics methods in identifying the temporal dependence of the data. Before continuing with the identification of the optimal parameters of the NARX network it was deemed necessary to examine whether these

713 exogenous inputs would improve the network's performance resulting in a NARX (nonlinear autoregressive
 714 method with exogenous inputs) architecture, or whether it would be preferred to only use the past values of the
 715 electricity demand as an input (NAR, nonlinear autoregressive method). The results of this analysis are depicted
 716 in **Figure 12.a** where it can be clearly seen that the temporal variables drastically improve the performance of the
 717 neural network especially for low feedback delays. For this reason, the NARX architecture was selected and a
 718 sensitivity analysis of the input and feedback delays as well as the number of neurons in the hidden layer was
 719 conducted. The results are depicted in **Figure 12.a-c** for each parameter, respectively. The performance of the
 720 neural network constantly improved until a certain point, as the number of input and feedback delays increased.
 721 The optimal values were identified 22 and 24 for the former and latter respectively. However, the number of
 722 neurons in the hidden layer did not seem to affect the performance of the network, and therefore the respective
 723 value was maintained at 12.



724

725

Figure 12. The sensitivity analysis and performance of ANN for electricity demand prediction

726 From the three predictive analytics methods used in this research, neural networks were the only ones that
 727 managed to achieve an overall good response for forecasting electricity demand which is depicted in **Figure 12.d**.
 728 The performance of the neural networks for each time horizon respectively is enlisted in **Table 17**. As expected
 729 the accuracy of the model drops as the time horizon of the prediction increases. **The forecasting error of the ANN**
 730 **model for predicting the electricity demand is reported in the fourth column of Table 9.**

731 **Table 17.** MSE values for various time horizons regarding solar power prediction with neural networks

| Time horizon | Mean Square Error |
|--------------|-------------------|
| model | 0.00079575 |
| 1-step | 0.00084579 |
| 2-step | 0.000931306 |
| 3-step | 0.001427005 |
| 4-step | 0.001738486 |
| 5-step | 0.00186682 |
| 6-step | 0.001882147 |

732

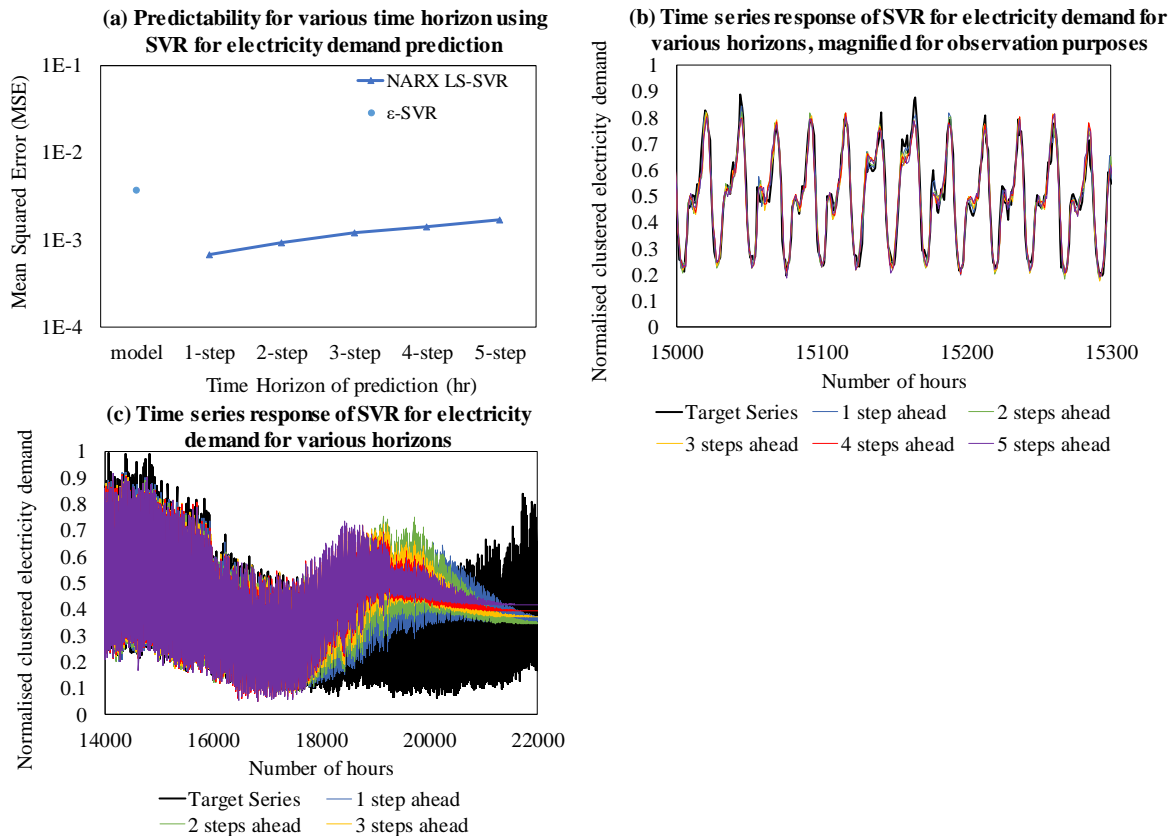
733 3.3.3. Support Vector Regression

734 Following the same approach as for the previous cases, the MATLAB toolbox of SVR was employed to study the
 735 response of the model for each of the three kernels, namely the linear, polynomial and the RBF. Similarly, it was
 736 found that the RBF kernel outperformed both others, and it was this kernel that was used therefore for the NARX
 737 LS-SVR. The testing performance of all the models computed are given in **Table 18** and are graphically
 738 represented in **Figure 13.a**.

739 The way with which the error increases for the case of electricity demand is remarkably different from the case
 740 of solar and wind prediction, since it does not seem to increase as steeply when the time horizon rises. This can
 741 be explained with **Figure 13.b** where it can be observed that overall the SVR failed to be trained successfully.
 742 Even though the right part of the response of **Figure 13.a-b** show promising results for a part of the data, at some
 743 point the model decays to a value. This signifies that perhaps the training data may not have been sufficient to
 744 make the model sensitive to the seasonal variations, or that after the data clustering the dataset should have been
 745 cleaned and any potential outliers ought to have been smoothed out. Nonetheless, it should be mentioned that the
 746 good response shown for parts of the forecasts displays the potential of SVRs to be used for this particular
 747 application.

Table 18. MSE values for various time horizons regarding electricity demand prediction with SVR

| Time horizon | Mean Square Error (Testing) |
|--------------------------|-----------------------------|
| Model (ϵ -SVR) | 0.0037 |
| 1-step (NARX LS-SVR) | 0.000677 |
| 2-step (NARX LS-SVR) | 0.000931 |
| 3-step (NARX LS-SVR) | 0.0012 |
| 4-step (NARX LS-SVR) | 0.0014 |
| 5-step (NARX LS-SVR) | 0.0017 |

**Figure 13.** The sensitivity analysis and performance of SVR for solar power prediction

753 3.3.4. Gaussian Regression Process (GPR)

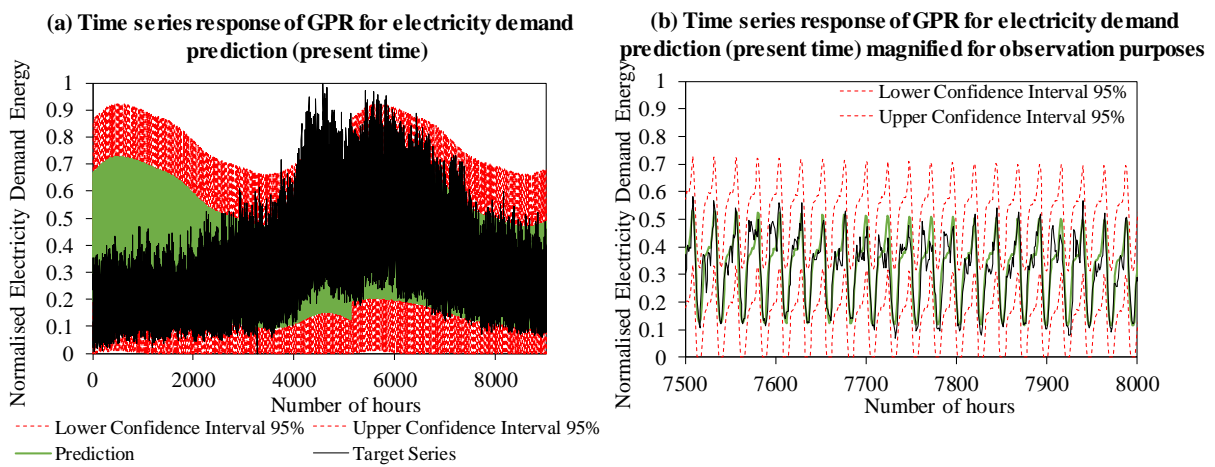
754 The Gaussian Regression Process, similar to SVR, was found also not to be able to capture the underlying patterns
 755 of the dataset of electricity demand. In **Table 19**, the performances retrieved from trying the various available
 756 kernels from the respective MATLAB toolbox can be seen. The training performances of all kernels other than
 757 the squared exponential and the ARD squared exponential were particularly high. The kernel that was selected
 758 was the squared exponential and the response of the model for the whole testing dataset is displayed in **Figure**
 759 **14.a** where it can be observed the model for a large part of the dataset does not follow the target series. In **Figure**

760 **14.b**, an area in which a good fitting was achieved is depicted and as for the method SVR, it is noted that this
 761 method has the potential of reaching a good accuracy.

762 **Table 19.** Sensitivity analysis for appropriate kernel function selection for electricity demand prediction

| Kernel function | Training Performance | Testing Performance |
|-------------------------|----------------------|---------------------|
| Squared exponential | 0.0106 | 0.0106 |
| Matern 32 | 1.0302 | 0.0105 |
| Matern 52 | 1.0301 | 0.0105 |
| ARD Squared Exponential | 0.0106 | 0.0106 |
| ARD Matern 32 | 1.0298 | 0.0104 |
| ARD Matern 52 | 1.0299 | 0.0105 |

763



764 **Figure 14.** (a) Time series response of GPR for electricity demand prediction (present time), (b) Time series response of
 765 GPR for electricity demand prediction (present time) magnified for observation purposes
 766
 767

768 3.4. Comparison of the prediction methods for wind and solar power as well as demand

769 In this section, all methods and types of predictions will be compared, with a view to summarise all the results
 770 presented above and to acquire an insight on the gains and limitations of each method tested. The comparison will
 771 be conducted on two levels. Firstly, the most suitable method will be identified for each type of prediction, and
 772 secondly the datasets will be compared for each machine-learning technique. **Figures 15a-c** depict the comparison
 773 of the models by graphing the mean square error of each model with the time horizon for which it was simulated
 774 while **Figures 15e-f** illustrate how each method has performed with regard to each dataset. The following points
 775 can be concluded:

- 776 • NARX LS-SVR outperforms NARX NN when the time horizon of the prediction is one, for all types of
 777 predictions.
- 778 • NARX NNs are found to be more robust for the case of wind power and solar power predictions as their
 779 decrease in accuracy is smaller than NARX LS-SVR. The opposite is observed for electricity demand.

- 780 • ϵ -SVR and GPR have similar errors for the cases of wind and solar power prediction. This signifies that if a
781 NARX GPR is implemented it is possible to gain satisfactory results.
- 782 • The poor performance of the GPR as well as of the ϵ -SVR (for wind and solar power) is attributed to the fact
783 that these models are not autoregressive, and utilise the target series only for supervised training and not as
784 an input.
- 785 • When looking at the electricity demand data, as time horizons of the predictions increase, the accuracy of
786 the models does not drop as in the respective cases of wind and solar power prediction. This denotes that the
787 initial error of the model is significant and the new error introduced by the predicting for longer periods of
788 time, contributes only slightly to the overall error.
- 789 • **Figures 15d-e** are similar which means that the wind and solar dataset behave in a similar manner with
790 regard to the various predictive models.

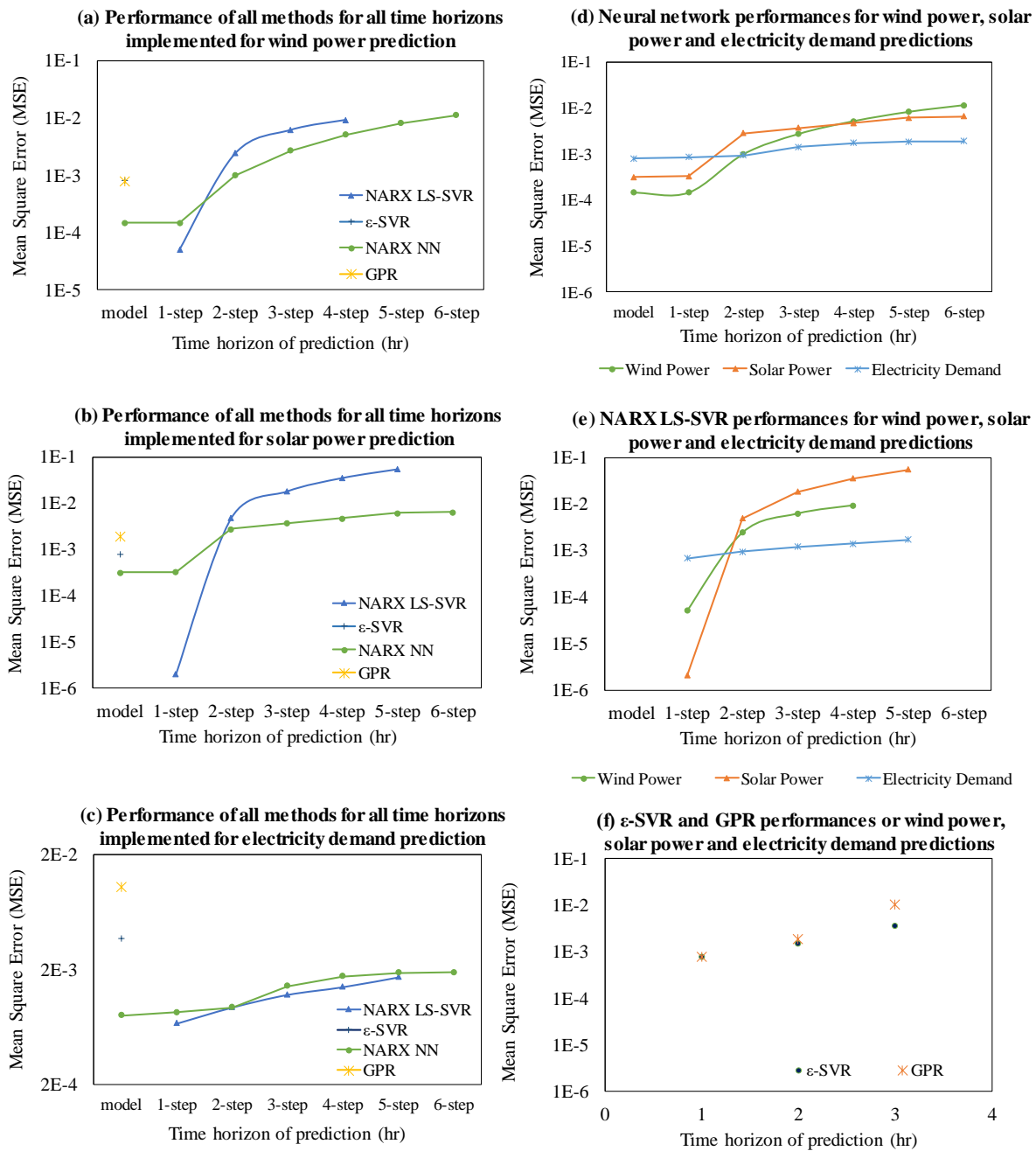


Figure 15. Comparison of the prediction methods for wind and solar power as well as demand

791

792

793

794

795

796

797

798

799

The best performing method built in this research was the NARX LS-SVR for one-hour ahead solar power prediction and the worst performing method was the GPR model for the case of demand. Even though the SVR and GPR models did not provide satisfactory results for the electricity demand prediction, it was shown that during some periods, the models managed to capture the underlying patterns of the data. This demonstrates that these particular methods are capable of potentially performing these predictions, however, certain measures must be taken in order to accomplish the desired outcome:

- 800 • More training data should be used with a view to provide the model more chances to understand the seasonal
801 variation of demand.
- 802 • The initial dataset of the 1157 households needs to be cleaned more thoroughly and include a step where the
803 outliers of the dataset are smoothed out. It is suggested the data is clustered and the resulting centroids should
804 be checked for outliers, and return to the initial data to perform smoothing with a view to cluster it again in
805 order to ensure that the outliers did not affect the classification of the data.
- 806 • The clustering of the data should be evaluated with further criteria other than the Silhouette coefficient
- 807 • Additional exogenous inputs should be introduced wherever possible. An example would be to include a
808 variable that denotes weekdays and weekends.
- 809 • If the steps above do not provide any significant improvements, a modelling tool could be used to extract
810 data with a view to establish whether the uncertainty and noise carried in the electricity demand dataset is
811 related to the failure of the prediction models.
- 812 • Finally, in **Table 20** and **Table 21** the mean square error of all the models is given. The green highlighting
813 denotes the method which has the best accuracy for each time horizon.

814 **Table 20.** Performance of all dynamic models

| Time Horizon | Wind Power | | Solar Power | | Electricity Demand | |
|-----------------|------------|----------|-------------|----------|--------------------|----------|
| | NN | SVR | NN | SVR | NN | SVR |
| 1 hour | 1.46E-04 | 5.03E-05 | 3.26E-04 | 2.03E-06 | 8.46E-04 | 6.7E-04 |
| 2 hours | 9.91E-04 | 2.4E-03 | 2.8E-03 | 4.9E-03 | 9.31E-04 | 9.31E-04 |
| 3 hours | 2.7E-03 | 6.2E-03 | 3.7E-03 | 1.82E-02 | 1.43E-03 | 1.2E-03 |
| 4 hours | 5.1E-03 | 9.3E-03 | 4.7E-03 | 3.56E-02 | 1.74E-03 | 1.4E-03 |
| 5 hours | 8.1E-03 | | 6.1E-03 | 5.51E-02 | 1.87E-03 | 1.7E-03 |
| 6 hours | 1.13E-02 | | 6.5E-03 | | 1.88E-03 | |

815

816 **Table 21.** Performance of all non-dynamic models

| Method | Wind Power | Solar Power | Electricity Demand |
|-----------------|------------|-------------|--------------------|
| NN | 1.45E-04 | 3.15E-04 | 7.97E-04 |
| ϵ -SVR | 7.97E-04 | 1.50E-03 | |
| GPR | 7.82E-04 | 1.90E-03 | 1.04E-02 |

817

818

819 3.5. Error Analysis and denormalization

820 With an aim to quantify the efficacy of the forecasting methods and the results of the predictive analysis, we
821 selected the best performing method for each of the time horizons and compared the error distributions with those
822 of a naive model, for wind power, solar power as well as electricity demand. Moreover, with a view to assessing
823 the impact of the mean errors to the forecasted values in a real-world application, the ranges of uncertainty have
824 been extrapolated to dimensional units. For the error analysis and specifically for the extrapolation of the error,
825 the following assumptions were made:

- 826 • Any fatigue factors or correlations to the age of the solar panels/ wind turbines is ignored.
- 827 • It is assumed that the predictive models are not influenced by the wind turbine model or the photovoltaic
828 types, respectively.
- 829 • Effects with regards to the interactions between the wind turbines are ignored.
- 830 • In the calculation of the mean capacity factor, no corrections were made to consider the periods in which the
831 wind turbines or solar photovoltaics are non-operational due to maintenance or other reasons.
- 832 • When extrapolating to calculate the expected generated energy along with the threshold of uncertainty, any
833 smoothing effects that may happen due to aggregation is ignored.
- 834 • The geographical variations in wind and solar availability, as well as electricity demand was formulated
835 according to a recent publications [173]. In that contribution, the availability of wind and solar energy was
836 clustered according into various geographical zones, and demand was considered according to its
837 demographical distribution.

838 The results of error percentage are shown in **Figure 16(a-c)** respectively, and denormalized in the following
839 sections. A comparison is also made with a naive model, for the sake illustration and clarification. The box plots
840 (also known as box and whisker diagram) in **Figure 16**, show six elements of the error distribution namely, the
841 minimum and maximum error, the first quartile, median, and third quartile, as well as the mean percentage errors
842 for each stochastic variable.

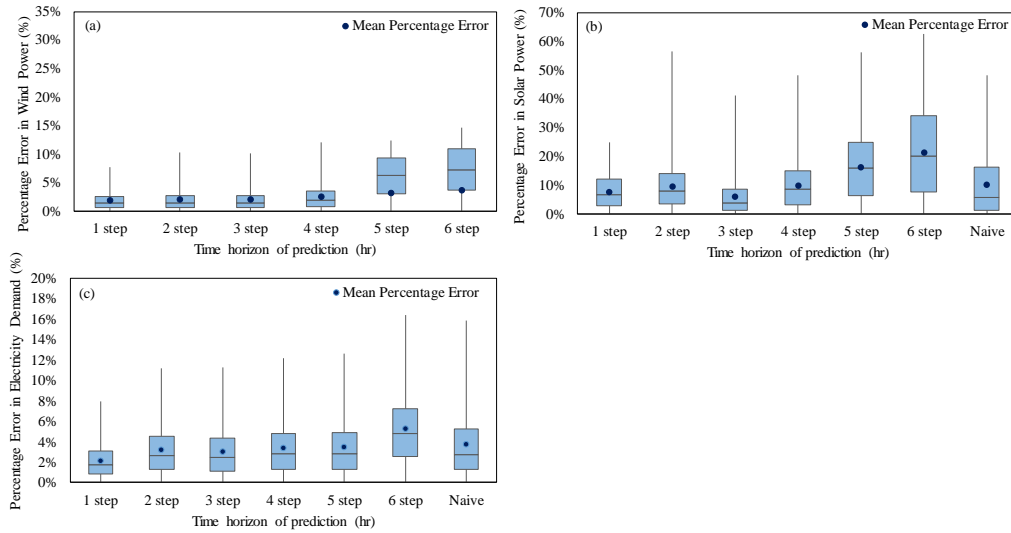


Figure 16. Box plot of percentage error distributions of (a) the wind power forecasting, (b) the solar power forecasting, (c) the electricity demand forecasting.

3.5.1. Error calculation of predictive models

The metric used for the error distribution analysis is the normalised root squared which is calculated as follows:

$$nrse = \frac{\sqrt{(y_{act} - y_{pr})^2}}{y_{act}} \quad (4)$$

where $nrse$ stands for normalised root square error. y_{act} and y_{pr} are the values of the actual and predicted performance respectively.

3.5.2. Naive Models

Naive models are used as a benchmark for comparison with the predictive models. Typically, it is expected that the predictive models outperform the naive models. For this work, two naive approaches were taken. For wind power which as prementioned (Table 7) has a low correlation with the time of day, for the naive approach, it is assumed that the energy produced at a given time horizon will be the same as the one at a given time earlier. More specifically:

$$y_{pr} = y_{t-i} \quad (5)$$

where y_{pr} is the resulting value of the naive model and y_{t-i} is the actual energy value at i hours before t .

On the other hand, solar power and electricity demand have a strong correlation to the time of day. Therefore, for the naive model, it is more appropriate to assume that the value at a given time horizon is the same as that of the respective time of the previous day.

$$y_{pr} = y_{t-24} \quad (6)$$

It is noted that whereas for wind power there are 6 naive models, for solar power and electricity demand only a single naive model is required.

866 **3.5.3. Wind Power**

867 **3.5.3.1. Error denormalization and distribution analysis**

868 In order to calculate the error of the wind prediction models in dimensional units, the output of the models is
 869 denormalised. The output of the wind forecasting models is the dimensionless power of a wind turbine. The data
 870 used for this research - as described in **Section 2.1, Table 4** - involved a particular model of a wind turbine at a
 871 hypothetical 1kW capacity. By denormalising the predictors' output and by looking at the error distributions of
 872 each of the predicted time horizons, **Figure 16(a)** shows the percentage error of the expected wind power of a
 873 wind turbine for a given time horizon. It should be noted that for the extraction of these, graphs outliers have been
 874 removed (errors that are greater or less than 3 standard deviations). The number of data points that were omitted
 875 for each case was at most 1.8%. In addition, the error distributions were calculated for the best performing model
 876 in each time horizon (see **Table 20**). In **Table 22** the respective results of the naive model can be seen. It is evident
 877 that as the time horizon increases the errors of the naive approach become increasing larger than the errors of the
 878 predictive forecasting methods. This means that the predictive models developed in this work add greater value
 879 in the increasing time horizons.

880 **Table 22.** The mean percentage error of naive and predictive model for wind power

| Time horizon (hr) | 1 step | 2 step | 3 step | 4 step | 5 step | 6 step |
|--------------------------|---------------|---------------|---------------|---------------|---------------|---------------|
| Naive Model | 1.76% | 3.38% | 4.82% | 6.12% | 7.27% | 8.31% |
| Predictive model | 1.88% | 2.05% | 2.04% | 2.61% | 3.17% | 3.73% |

881
 882 **3.5.3.2. Quantification of errors in dimensional units.**

883 In this section, the uncertainty of the wind power predictions will be quantified for a Vestas V80 2000 wind
 884 turbine and will be extrapolated at a national level (UK). The range of uncertainty will be given for the generated
 885 energy that corresponds to the mean capacity factor of a wind turbine in the UK. The mean capacity factor of
 886 onshore wind farms can be estimated with the following calculation:

887
$$cf_{wind} = \frac{Generated\ Energy_{2017}}{Capacity_{2017} * 24 * 365} \quad (7)$$

888 where $Generated\ Energy_{2017}$ refers to the total power generated from onshore wind farms in 2017 and
 889 $Capacity_{2017}$ is the total capacity of onshore wind farms in 2017. Since the capacity of wind power is ever
 890 increasing and therefore not a constant value throughout the year, we assume that the new onshore wind farms in
 891 2017 were introduced to the grid evenly across the year.

892
$$Capacity_{2017} = TotalCapacity_{2017} - \left(\frac{TotalCapacity_{2017} - TotalCapacity_{2016}}{2} \right) = 30.52\% \quad (8)$$

893 **Table 23.** The capacity of and electricity generated from onshore wind farms in the UK [174]

| | |
|---|-----------|
| Total generated energy from onshore wind farms in the UK for 2017 | 29088 GWh |
| Total onshore wind farm capacity at the end of 2017 | 12847 MW |
| Total onshore wind farm capacity at the end of 2016 | 10880 MW |

894

895 Using the values in **Table 23** [174] the mean capacity factor is estimated to be 30.52%. In **Table 24**, the estimated
 896 generated energy for a given hour of a Vestas V80 2000 wind turbine, and of the entire UK onshore wind farm
 897 fleet have been calculated.

898 **Table 24.** The mean percentage error of naive and predictive model for wind power generation for an hour

| | Model Type | 1 step | 2 step | 3 step | 4 step | 5 step | 6 step |
|--------------------|------------------|-------------|-------------|-------------|-------------|-------------|-------------|
| Wind Turbine [KWh] | Naive Model | 610.4 ±10.7 | 610.4 ±20.6 | 610.4 ±29.4 | 610.4 ±37.3 | 610.4 ±44.3 | 610.4 ±50.7 |
| Wind Turbine [KWh] | Predictive model | 610.4 ±11.5 | 610.4 ±12.5 | 610.4 ±12.4 | 610.4 ±15.9 | 610.4 ±19.3 | 610.4 ±22.8 |
| UK (2017) [MWh] | Naive Model | 3921±69.0 | 3921±132.5 | 3921±189.0 | 3921±240.0 | 3921±285.1 | 3921±325.8 |
| UK (2017) [MWh] | Predictive model | 3921±73.7 | 3921±80.4 | 3921±80.0 | 3921±102.3 | 3921±124.3 | 3921±146.3 |

899

900 3.5.4. Solar Power

901 3.5.4.1. Error denormalization and distribution analysis

902 In a similar manner to wind power, the outputs of the solar prediction models are denormalised and the percentage
 903 root squared error distribution is calculated (**Table 25** and **Figure 16(b)**). It should be noted that for the error
 904 distribution analysis, only values during daylight were considered. It can be seen that the naive approach
 905 outperforms the predictive models for time horizons greater than 4 hours. This indicates that better forecasting
 906 performances may have been achieved if the energy produced on the previous day at the same time was used as
 907 an input.

908 **Table 25.** Mean percentage error of naive and predictive model for solar power

| Model Type | Mean percentage error |
|------------|-----------------------|
| 1 step | 7.86% |
| 2 step | 9.66% |
| 3 step | 6.10% |
| 4 step | 10.17% |
| 5 step | 16.48% |
| 6 step | 21.41% |
| Naive | 10.38% |

909

910 3.5.4.2. Quantification of errors in dimensional units.

911 In this section, the uncertainty of the solar power predictions will be quantified for a solar power farm of 200 MW,
 912 and will be extrapolated at a national level (UK). Similar to the section above, the mean capacity factor is estimated
 913 to be 10.66%, given the values of **Table 26**. The mean percentage error of naive and predictive model are reported
 914 in **Table 27**.

915 **Table 26.** The capacity of and electricity generated from solar photovoltaic farms in the UK [174]

| | |
|---|-----------|
| Total generated energy from onshore wind farms in the UK for 2017 | 11525 GWh |
| Total onshore wind farm capacity at the end of 2017 | 12776 MW |
| Total onshore wind farm capacity at the end of 2016 | 11912 MW |

916

917

918 **Table 27.** Mean percentage error of naive and predictive model for solar power for an hour

| | 1 step | 2 step | 3 step | 4 step | 5 step | 6 step | Naive |
|------------------|---------------|---------------|---------------|---------------|---------------|---------------|--------------|
| Solar Farm [MWh] | 21.3 ±1.68 | 21.3 ±2.06 | 21.3 ±1.3 | 21.3 ±2.17 | 21.3 ±3.51 | 21.3 ±4.56 | 21.3 ±2.21 |
| UK (2017) [MWh] | 1362±107 | 1362±132 | 1362±83 | 1362±139 | 1362±225 | 1362±292 | 1362±141 |

919

920

921 **3.5.5. Electricity Demand**

922 **3.5.5.1. Error denormalization and distribution analysis**

923 The output of the electricity demand models is the normalised energy spent in a household for a given hour. The
924 distribution of the percentage error is presented in **Figure 16(c)**, and the mean values of the error are given in
925 **Table 28**. As in the case of solar power generation, it can be observed that the performance of the naive model is
926 relatively good. This indicates that for the 6 hours ahead prediction, better forecasting performances could be
927 achieved if the energy produced on the previous day at the same time was used as an input.

928 **Table 28.** Mean percentage error of naive and predictive model for electricity demand

| Model Type | Mean percentage error |
|------------|-----------------------|
| 1 step | 2.10% |
| 2 step | 3.13% |
| 3 step | 3.00% |
| 4 step | 3.31% |
| 5 step | 3.40% |
| 6 step | 5.20% |
| Naive | 3.67% |

929

930 **3.5.5.2. Quantification of errors in dimensional units**

931 With a view to quantifying the errors in dimensional units for domestic electricity demand, the energy usage will
932 be extrapolated to that of an average household in the UK. According to [175] looking at the average hourly load
933 curves of households without electricity heating the peak load typically reaches 600W (**Table 29**).

934 **Table 29.** Mean percentage error of the naive and predictive models for the electricity consumption of an
935 average household without electricity heating.

| | 1 step | 2 step | 3 step | 4 step | 5 step | 6 step | Naive |
|---|------------|------------|---------|------------|------------|------------|------------|
| Household consumption during peak time for 1hr [Wh] | 600 ±12.59 | 600 ±18.79 | 600 ±18 | 600 ±19.84 | 600 ±20.41 | 600 ±31.21 | 600 ±22.01 |

936

937 **4. Conclusions**

938 This research has successfully implemented predictive analytics methods that forecast the wind power, the solar
939 power and the electricity demand of households. Moreover, the uncertainty of these predictions is quantified by
940 the mean square error for the case of neural networks and support vector regression, as well as confidence intervals
941 for the Gaussian process regression method. It is believed that from the knowledge acquired by these data-driven
942 models an optimal investment and usage of energy storage units could be achieved, which would result in
943 achieving an economically feasible solution that allows an even higher level of penetration of renewable energy
944 sources within an electricity grid.

945 Finally, it should be mentioned that there are many additional opportunities and issues that need to be addressed,
946 when looking at the future of the energy sector. For example, demand-side response, where incentives are given
947 to customers to use electricity at off-peak hours has shown to have a very beneficial effect in managing and
948 controlling the load of the electricity grid. With the increase of electric vehicles, demand-side response can gain
949 an even greater role in the electricity distribution system. The batteries of the cars that are interconnected to the
950 grid in an event of a frequency drop can provide electricity to the grid instead of charging, thus avoiding the
951 immediate conventional plant response [176]. All these opportunities should be integrated within a predictive
952 control system for a smart grid and it is evident that the results of such research can be immediately applicable
953 and can facilitate and contribute to the transition of the energy sector to modern and sustainable technologies.

954

955 **Acknowledgment**

956 The measurements data of electricity demand was provided by the Hildebrand Technology limited, which is
957 gratefully acknowledged.

958

959 **Abbreviations**

| | |
|-------|---|
| ANFIS | Adaptive Neuro Fuzzy Inference System |
| ANN | Artificial Neural Networks |
| AR | AutoRegressive |
| ARCH | AutoRegressive Conditional Heteroskedasticity model |
| ARIMA | AutoRegressive Integrated Moving Average |
| ARMA | AutoRegressive Moving Average |
| BIC | Bayesian Information Critetion |
| BP | Back Propagation Neural Network |
| BR | Bayesian Regularisation |
| ELM | Elman Recurrent Neural Network |
| EXS | Exponential Smoothing |
| FIR | Finite Impulse Response Neural Network |
| FLS | Fuzzy Logic Systems |
| FNN | Fuzzy Neural Network |
| GA | Genetic Algorithm |
| GHGs | Greenhouse gases |
| GPR | Gaussian Regression Process |
| ICA | Imperialist Component Algorithm |
| IEA | International Energy Agency |
| I-O | Input-Output model |
| kNN | k-Nearest Neighbour |
| LM | Levenberg-Marquart |

| | |
|--------|--|
| LS-SVR | Least Squared Support Vector Regression |
| MA | Moving Average |
| ME | Mixture of Experts |
| MLP | Multilayer Perceptron Neural Network |
| MPC | Model Predictive Control |
| NAR | Nonlinear AutoRegressive model |
| NARX | Nonlinear AutoRegressive model with eXogenous inputs |
| NLN | Neural Logic Network |
| NNS | Nearest Neighbour Search |
| NWP | Numerical Weather Prediction |
| PCA | Principal Component Analysis |
| PV | PhotoVoltaic |
| SCADA | Supervisory Control and Data Acquisition |
| QR | Quantile Regression |
| QRF | Quantile Random Forest |
| RBF | Radial Base Function Neural Network |
| RES | renewable energy resources |
| RF | Random Forest |
| SRN | Simultaneous Recurrent Neural Network |
| SVM | Support Vector Machines |
| SVR | Support Vector Regression |

960

961 **References**

- 962 [1] International Energy Agency, IEA. Energy and Climate Change. Paris, France: 2015.
963 doi:10.1038/479267b.
- 964 [2] Tayal D. Achieving high renewable energy penetration in Western Australia using data digitisation and
965 machine learning. *Renew Sustain Energy Rev* 2017;80:1537–43. doi:10.1016/j.rser.2017.07.040.
- 966 [3] Suganthi L, Samuel AA. Energy models for demand forecasting—A review. *Renew Sustain Energy Rev*
967 2012;16:1223–40. doi:10.1016/j.rser.2011.08.014.
- 968 [4] Khan AR, Mahmood A, Safdar A, Khan ZA, Khan NA. Load forecasting, dynamic pricing and DSM in
969 smart grid: A review. vol. 54. Elsevier; 2016. doi:10.1016/j.rser.2015.10.117.
- 970 [5] Mellit A, Kalogirou S a. Artificial intelligence techniques for photovoltaic applications: A review. *Prog*
971 *Energy Combust Sci* 2008;34:574–632. doi:10.1016/j.pecs.2008.01.001.
- 972 [6] Inman RH, Pedro HTC, Coimbra CFM. Solar forecasting methods for renewable energy integration. *Prog*
973 *Energy Combust Sci* 2013;39:535–76. doi:10.1016/j.pecs.2013.06.002.
- 974 [7] Jung J, Broadwater RP. Current Status and Future Advances for Wind Speed and Power Forecasting.
975 *Renew Sustain Energy Rev* 2014;31:762–77. doi:10.1016/j.rser.2013.12.054.

- 976 [8] Baños R, Manzano-Agugliaro F, Montoya FG, Gil C, Alcayde A, Gómez J. Optimization methods applied
977 to renewable and sustainable energy: A review. *Renew Sustain Energy Rev* 2011;15:1753–66.
978 doi:10.1016/j.rser.2010.12.008.
- 979 [9] Sfetsos A. A comparison of various forecasting techniques applied to mean hourly wind speed time series.
980 *Renew Energy* 2000;21:23–35. doi:10.1016/S0960-1481(99)00125-1.
- 981 [10] Martín L, Zarzalejo LF, Polo J, Navarro A, Marchante R, Cony M. Prediction of global solar irradiance
982 based on time series analysis: Application to solar thermal power plants energy production planning. *Sol*
983 *Energy* 2010;84:1772–81. doi:10.1016/j.solener.2010.07.002.
- 984 [11] Fernandez-Jimenez LA, Muñoz-Jimenez A, Falces A, Mendoza-Villena M, Garcia-Garrido E, Lara-
985 Santillan PM, et al. Short-term power forecasting system for photovoltaic plants. *Renew Energy*
986 2012;44:311–7. doi:10.1016/j.renene.2012.01.108.
- 987 [12] Costa A, Crespo A, Navarro J, Lizcano G, Madsen H, Feitosa E. A review on the young history of the
988 wind power short-term prediction. *Renew Sustain Energy Rev* 2008;12:1725–44.
989 doi:10.1016/j.rser.2007.01.015.
- 990 [13] Salcedo-Sanz S, Cornejo-Bueno L, Prieto L, Paredes D, García-Herrera R. Feature selection in machine
991 learning prediction systems for renewable energy applications. *Renew Sustain Energy Rev* 2018;90:728–
992 41. doi:10.1016/j.rser.2018.04.008.
- 993 [14] Zheng ZW, Chen YY, Huo MM, Zhao B. An Overview: the Development of Prediction Technology of
994 Wind and Photovoltaic Power Generation. *Energy Procedia* 2011;12:601–8.
995 doi:10.1016/j.egypro.2011.10.081.
- 996 [15] Shi J, Qu X, Zeng S. Short-Term Wind Power Generation Forecasting: Direct Versus Indirect Arima-
997 Based Approaches. *Int J Green Energy* 2011;8:100–12. doi:10.1080/15435075.2011.546755.
- 998 [16] Kusiak A, Zheng H, Song Z. Short-term prediction of wind farm power: A data mining approach. *IEEE*
999 *Trans Energy Convers* 2009;24:125–36. doi:10.1109/TEC.2008.2006552.
- 1000 [17] Sánchez I. Short-term prediction of wind energy production. *Int J Forecast* 2006;22:43–56.
1001 doi:10.1016/j.ijforecast.2005.05.003.
- 1002 [18] Meng A, Ge J, Yin H, Chen S. Wind speed forecasting based on wavelet packet decomposition and
1003 artificial neural networks trained by crisscross optimization algorithm. *Energy Convers Manag*
1004 2016;114:75–88. doi:10.1016/J.ENCONMAN.2016.02.013.
- 1005 [19] Liu H, Mi X, Li Y. Wind speed forecasting method based on deep learning strategy using empirical

- 1006 wavelet transform, long short term memory neural network and Elman neural network. *Energy Convers*
1007 *Manag* 2018;156:498–514.
- 1008 [20] Wang HZ, Wang GB, Li GQ, Peng JC, Liu YT. Deep belief network based deterministic and probabilistic
1009 wind speed forecasting approach. *Appl Energy* 2016;182:80–93.
1010 doi:10.1016/J.APENERGY.2016.08.108.
- 1011 [21] Wang H, Li G, Wang G, Peng J, Jiang H, Liu Y. Deep learning based ensemble approach for probabilistic
1012 wind power forecasting. *Appl Energy* 2017;188:56–70.
- 1013 [22] Yu J, Chen K, Mori J, Rashid MM. A Gaussian mixture copula model based localized Gaussian process
1014 regression approach for long-term wind speed prediction. *Energy* 2013;61:673–86.
1015 doi:10.1016/J.ENERGY.2013.09.013.
- 1016 [23] Yu R, Gao J, Yu M, Lu W, Xu T, Zhao M, et al. LSTM-EFG for wind power forecasting based on
1017 sequential correlation features. *Futur Gener Comput Syst* 2019;93:33–42.
1018 doi:10.1016/J.FUTURE.2018.09.054.
- 1019 [24] Liu H, Mi X, Li Y. Smart deep learning based wind speed prediction model using wavelet packet
1020 decomposition, convolutional neural network and convolutional long short term memory network. *Energy*
1021 *Convers Manag* 2018;166:120–31. doi:10.1016/j.enconman.2018.04.021.
- 1022 [25] Liu H, Mi X, Li Y. Smart multi-step deep learning model for wind speed forecasting based on variational
1023 mode decomposition, singular spectrum analysis, LSTM network and ELM. *Energy Convers Manag*
1024 2018;159:54–64. doi:10.1016/j.enconman.2018.01.010.
- 1025 [26] Zhu A, Li X, Mo Z, Wu H. Wind power prediction based on a convolutional neural network. 2017 Int
1026 Conf Circuits, Devices Syst ICCDS 2017 2017;2017–Janua:131–5. doi:10.1109/ICCDs.2017.8120465.
- 1027 [27] Hu YL, Chen L. A nonlinear hybrid wind speed forecasting model using LSTM network, hysteretic ELM
1028 and Differential Evolution algorithm. *Energy Convers Manag* 2018;173:123–42.
1029 doi:10.1016/j.enconman.2018.07.070.
- 1030 [28] Wang J, Li Y. Multi-step ahead wind speed prediction based on optimal feature extraction, long short
1031 term memory neural network and error correction strategy. *Appl Energy* 2018;230:429–43.
1032 doi:10.1016/j.apenergy.2018.08.114.
- 1033 [29] Wang K, Qi X, Liu H, Song J. Deep belief network based k-means cluster approach for short-term wind
1034 power forecasting. *Energy* 2018;165:840–52. doi:10.1016/j.energy.2018.09.118.
- 1035 [30] Zhang Y, Le J, Liao X, Zheng F, Li Y. A novel combination forecasting model for wind power integrating

- 1036 least square support vector machine, deep belief network, singular spectrum analysis and locality-sensitive
1037 hashing. *Energy* 2018;168:558–72. doi:10.1016/j.energy.2018.11.128.
- 1038 [31] Yu C, Li Y, Bao Y, Tang H, Zhai G. A novel framework for wind speed prediction based on recurrent
1039 neural networks and support vector machine. *Energy Convers Manag* 2018;178:137–45.
1040 doi:10.1016/j.enconman.2018.10.008.
- 1041 [32] Higashiyama K, Fujimoto Y, Hayashi Y. Feature Extraction of NWP Data for Wind Power Forecast by
1042 Using 3D-Convolutional Neural Network. *12th Int Renew Energy Storage Conf* 2018;155:350–8.
1043 doi:10.1016/J.EGYPRO.2018.11.043.
- 1044 [33] Chen J, Zeng GQ, Zhou W, Du W, Lu K Di. Wind speed forecasting using nonlinear-learning ensemble
1045 of deep learning time series prediction and extremal optimization. *Energy Convers Manag* 2018;165:681–
1046 95. doi:10.1016/j.enconman.2018.03.098.
- 1047 [34] Chen N, Qian Z, Nabney IT, Meng X. Wind power forecasts using gaussian processes and numerical
1048 weather prediction. *IEEE Trans Power Syst* 2014;29:656–65. doi:10.1109/TPWRS.2013.2282366.
- 1049 [35] Jiang X, Dong B, Xie L, Sweeney L. Adaptive Gaussian Process for Short-Term Wind Speed Forecasting
1050 2010.
- 1051 [36] Ernst B, Oakleaf B, Ahlstrom ML, Lange M, Moehrlen C, Lange B, et al. Predicting the wind. *IEEE*
1052 *Power Energy Mag* 2007;5:78–89. doi:10.1109/MPE.2007.906306.
- 1053 [37] Hu J, Heng J, Tang J, Guo M. Research and application of a hybrid model based on Meta learning strategy
1054 for wind power deterministic and probabilistic forecasting. *Energy Convers Manag* 2018;173:197–209.
1055 doi:10.1016/j.enconman.2018.07.052.
- 1056 [38] Barbosa de Alencar D, de Mattos Affonso C, Limão de Oliveira R, Moya Rodríguez J, Leite J, Reston
1057 Filho J. Different Models for Forecasting Wind Power Generation: Case Study. *Energies* 2017;10:1976.
1058 doi:10.3390/en10121976.
- 1059 [39] Tascikaraoglu A, Uzunoglu M. A review of combined approaches for prediction of short-term wind speed
1060 and power. *Renew Sustain Energy Rev* 2014;34:243–54. doi:10.1016/j.rser.2014.03.033.
- 1061 [40] Foley AM, Leahy PG, Marvuglia A, McKeogh EJ. Current methods and advances in forecasting of wind
1062 power generation. *Renew Energy* 2012;37:1–8. doi:10.1016/j.renene.2011.05.033.
- 1063 [41] Ak R, Vitelli V, Zio E. An Interval-Valued Neural Network Approach for Prediction Uncertainty
1064 Quantification. *IEEE Trans Neural Networks Learn Syst* 2015;26:2787–800.
1065 doi:10.1109/TNNLS.2015.2396933.

- 1066 [42] Masseran N. Modeling the fluctuations of wind speed data by considering their mean and volatility effects.
1067 Renew Sustain Energy Rev 2016;54:777–84. doi:10.1016/j.rser.2015.10.071.
- 1068 [43] Alexiadis MC, Dokopoulos PS, Sahsamanoglou HS, Manousaridis IM. Short-term forecasting of wind
1069 speed and related electrical power. Sol Energy 1998;63:61–8. doi:10.1016/S0038-092X(98)00032-2.
- 1070 [44] Sideratos G, Hatziaargyriou ND. An Advanced Statistical Method for Wind Power Forecasting. Power
1071 Syst IEEE Trans 2007;22:258–65. doi:10.1109/tpwrs.2006.889078.
- 1072 [45] Mohandes MA, Halawani TO, Rehman S, Hussain AA. Support vector machines for wind speed
1073 prediction. Renew Energy 2004;29:939–47. doi:10.1016/j.renene.2003.11.009.
- 1074 [46] Jursa R, Rohrig K. Short-term wind power forecasting using evolutionary algorithms for the automated
1075 specification of artificial intelligence models. Int J Forecast 2008;24:694–709.
1076 doi:10.1016/j.ijforecast.2008.08.007.
- 1077 [47] Ghadi MJ, Gilani SH, Afrakhte H, Baghrmian A. A novel heuristic method for wind farm power
1078 prediction: A case study. Int J Electr Power Energy Syst 2014;63:962–70.
1079 doi:10.1016/j.ijepes.2014.07.008.
- 1080 [48] Kramer O, Gieseke F. Short-term wind energy forecasting using support vector regression. Soft Comput
1081 Model Ind Environ Appl 6th Int Conf SOCO 2011 2011;87:271–80. doi:10.1007/978-3-642-19644-7_29.
- 1082 [49] Han S, Li J, Liu Y. Tabu Search Algorithm Optimized ANN Model for Wind Power Prediction with NWP.
1083 Energy Procedia 2011;12:733–40. doi:10.1016/j.egypro.2011.10.099.
- 1084 [50] Carolin Mabel M, Fernandez E. Analysis of wind power generation and prediction using ANN: A case
1085 study. Renew Energy 2008;33:986–92. doi:10.1016/j.renene.2007.06.013.
- 1086 [51] Cellura M, Cirrincione G, Marvuglia A, Miraoui A. Wind speed spatial estimation for energy planning in
1087 {Sicily}: {A} neural kriging application. Renew Energy 2008;33:1251–66.
1088 doi:10.1016/j.renene.2007.08.013.
- 1089 [52] Welch RL, Ruffing SM, Venayagamoorthy GK. Comparison of Feedforward and Feedback Neural
1090 Network Architectures for Short Term Wind Speed Prediction. Proc Int Jt Conf Neural Networks
1091 2009:3335–40. doi:10.1109/IJCNN.2009.5179034.
- 1092 [53] Ramirez-Rosado IJ, Fernandez-Jimenez LA, Monteiro C, Sousa J, Bessa R. Comparison of two new short-
1093 term wind-power forecasting systems. Renew Energy 2009;34:1848–54.
1094 doi:10.1016/j.renene.2008.11.014.
- 1095 [54] Bin S, Haitao Y, Ting L. Short-term Wind Speed Forecasting Based on Gaussian Process Regression

- 1096 Model. CSEE, 2012.
- 1097 [55] Hong T, Pinson P, Fan S. Global energy forecasting competition 2012. *Int J Forecast* 2014;30:357–63.
1098 doi:10.1016/j.ijforecast.2013.07.001.
- 1099 [56] Barbounis TG, Theocharis JB. Locally recurrent neural networks for wind speed prediction using spatial
1100 correlation. *Inf Sci (Ny)* 2007;177:5775–97. doi:10.1016/j.ins.2007.05.024.
- 1101 [57] Eseye AT, Zhang J, Zheng D, Ma H, Jingfu G. Short-term wind power forecasting using a double-stage
1102 hierarchical hybrid GA-ANN approach. 2017 IEEE 2nd Int. Conf. Big Data Anal. (ICBDA)(, IEEE; 2017,
1103 p. 552–6. doi:10.1109/ICBDA.2017.8078695.
- 1104 [58] Najeebullah, Zameer A, Khan A, Javed SG. Machine Learning based short term wind power prediction
1105 using a hybrid learning model. *Comput Electr Eng* 2015;45:122–33.
1106 doi:10.1016/j.compeleceng.2014.07.009.
- 1107 [59] Li C, Lin S, Xu F, Liu D, Liu J. Short-term wind power prediction based on data mining technology and
1108 improved support vector machine method: A case study in Northwest China. vol. 205. Elsevier Ltd; 2018.
1109 doi:10.1016/j.jclepro.2018.09.143.
- 1110 [60] Bacher P, Madsen H, Nielsen HA. Online short-term solar power forecasting. *Sol Energy* 2009;83:1772–
1111 83.
- 1112 [61] Troncoso A, Salcedo-Sanz S, Casanova-Mateo C, Riquelme JC, Prieto L. Local models-based regression
1113 trees for very short-term wind speed prediction. *Renew Energy* 2015;81:589–98.
1114 doi:10.1016/J.RENENE.2015.03.071.
- 1115 [62] Pedro HTC, Coimbra CFM. Assessment of forecasting techniques for solar power production with no
1116 exogenous inputs. *Sol Energy* 2012;86:2017–28.
- 1117 [63] Pedro HTC, Coimbra CFM, David M, Lauret P. Assessment of machine learning techniques for
1118 deterministic and probabilistic intra-hour solar forecasts. *Renew Energy* 2018;123:191–203.
- 1119 [64] Tang P, Chen D, Hou Y. Entropy method combined with extreme learning machine method for the short-
1120 term photovoltaic power generation forecasting. *Chaos, Solitons & Fractals* 2016;89:243–8.
1121 doi:10.1016/J.CHAOS.2015.11.008.
- 1122 [65] Paoli C, Voyant C, Muselli M, Nivet M-L. Forecasting of preprocessed daily solar radiation time series
1123 using neural networks. *Sol Energy* 2010;84:2146–60. doi:10.1016/J.SOLENER.2010.08.011.
- 1124 [66] Lauret P, Voyant C, Soubdhan T, David M, Poggi P. A benchmarking of machine learning techniques for
1125 solar radiation forecasting in an insular context. *Sol Energy* 2015;112:446–57.

- 1126 doi:10.1016/J.SOLENER.2014.12.014.
- 1127 [67] Bouzerdoum M, Mellit A, Massi Pavan A. A hybrid model (SARIMA–SVM) for short-term power
1128 forecasting of a small-scale grid-connected photovoltaic plant. *Sol Energy* 2013;98:226–35.
1129 doi:10.1016/J.SOLENER.2013.10.002.
- 1130 [68] Sheng H, Xiao J, Cheng Y, Ni Q, Wang S. Short-Term Solar Power Forecasting Based on Weighted
1131 Gaussian Process Regression. *IEEE Trans Ind Electron* 2018. doi:10.1109/TIE.2017.2714127.
- 1132 [69] Salcedo-Sanz S, Casanova-Mateo C, Munoz-Mari J, Camps-Valls G. Prediction of Daily Global Solar
1133 Irradiation Using Temporal Gaussian Processes. *IEEE Geosci Remote Sens Lett* 2014;11:1936–40.
1134 doi:10.1109/LGRS.2014.2314315.
- 1135 [70] Reikard G. Predicting solar radiation at high resolutions: A comparison of time series forecasts. *Sol*
1136 *Energy* 2009;83:342–9. doi:10.1016/j.solener.2008.08.007.
- 1137 [71] Behera MK, Majumder I, Nayak N. Solar photovoltaic power forecasting using optimized modified
1138 extreme learning machine technique. *Eng Sci Technol an Int J* 2018;21:428–38.
1139 doi:10.1016/J.JESTCH.2018.04.013.
- 1140 [72] Sharma A, Kakkar A. Forecasting daily global solar irradiance generation using machine learning. *Renew*
1141 *Sustain Energy Rev* 2018;82:2254–69. doi:10.1016/J.RSER.2017.08.066.
- 1142 [73] Hossain M, Mekhilef S, Danesh M, Olatomiwa L, Shamshirband S. Application of extreme learning
1143 machine for short term output power forecasting of three grid-connected PV systems. *J Clean Prod*
1144 2017;167:395–405.
- 1145 [74] Majumder I, Dash PK, Bisoi R. Variational mode decomposition based low rank robust kernel extreme
1146 learning machine for solar irradiation forecasting. *Energy Convers Manag* 2018;171:787–806.
1147 doi:10.1016/J.ENCONMAN.2018.06.021.
- 1148 [75] Srivastava S, Lessmann S. A comparative study of LSTM neural networks in forecasting day-ahead global
1149 horizontal irradiance with satellite data. *Sol Energy* 2018;162:232–47.
1150 doi:10.1016/J.SOLENER.2018.01.005.
- 1151 [76] Qing X, Niu Y. Hourly day-ahead solar irradiance prediction using weather forecasts by LSTM. *Energy*
1152 2018;148:461–8. doi:10.1016/j.energy.2018.01.177.
- 1153 [77] Alzahrani A, Shamsi P, Dagli C, Ferdowsi M. Solar Irradiance Forecasting Using Deep Neural Networks.
1154 *Procedia Comput Sci* 2017;114:304–13. doi:10.1016/j.procs.2017.09.045.
- 1155 [78] Li LL, Cheng P, Lin HC, Dong H. Short-term output power forecasting of photovoltaic systems based on

- 1156 the deep belief net. *Adv Mech Eng* 2017;9:1–13. doi:10.1177/1687814017715983.
- 1157 [79] Abdel-Nasser M, Mahmoud K. Accurate photovoltaic power forecasting models using deep LSTM-RNN.
1158 *Neural Comput Appl* 2017:1–14. doi:10.1007/s00521-017-3225-z.
- 1159 [80] Zhang J, Verschae R, Nobuhara S, Lalonde J-FF. Deep photovoltaic nowcasting. *Sol Energy*
1160 2018;176:267–76. doi:10.1016/j.solener.2018.10.024.
- 1161 [81] Wang H, Yi H, Peng J, Wang G, Liu Y, Jiang H, et al. Deterministic and probabilistic forecasting of
1162 photovoltaic power based on deep convolutional neural network. *Energy Convers Manag* 2017;153:409–
1163 22. doi:10.1016/j.enconman.2017.10.008.
- 1164 [82] Ridley B, Boland J, Lauret P. Modelling of diffuse solar fraction with multiple predictors. *Renew Energy*
1165 2010;35:478–83. doi:10.1016/j.renene.2009.07.018.
- 1166 [83] Ruiz-Arias JA, Alsamamra H, Tovar-Pescador J, Pozo-Vázquez D. Proposal of a regressive model for the
1167 hourly diffuse solar radiation under all sky conditions. *Energy Convers Manag* 2010;51:881–93.
1168 doi:10.1016/j.enconman.2009.11.024.
- 1169 [84] Chen C, Duan S, Cai T, Liu B. Online 24-h solar power forecasting based on weather type classification
1170 using artificial neural network. *Sol Energy* 2011;85:2856–70. doi:10.1016/j.solener.2011.08.027.
- 1171 [85] İzgi E, Öztöpal A, Yerli B, Kaymak MK, Şahin AD. Short–mid-term solar power prediction by using
1172 artificial neural networks. *Sol Energy* 2012;86:725–33. doi:10.1016/j.solener.2011.11.013.
- 1173 [86] Mellit A, Pavan AM. A 24-h forecast of solar irradiance using artificial neural network: Application for
1174 performance prediction of a grid-connected PV plant at Trieste, Italy. *Sol Energy* 2010;84:807–21.
1175 doi:10.1016/j.solener.2010.02.006.
- 1176 [87] Mellit A, Benghane M, Kalogirou SA. Modeling and simulation of a stand-alone photovoltaic system
1177 using an adaptive artificial neural network: Proposition for a new sizing procedure. *Renew Energy*
1178 2007;32:285–313. doi:10.1016/j.renene.2006.01.002.
- 1179 [88] Mellit A, Eleuch H, Benghane M, Elaoun C, Pavan AM. An adaptive model for predicting of global,
1180 direct and diffuse hourly solar irradiance. *Energy Convers Manag* 2010;51:771–82.
1181 doi:10.1016/j.enconman.2009.10.034.
- 1182 [89] Shi J, Lee WJ, Liu Y, Yang Y, Wang P. Forecasting power output of photovoltaic systems based on
1183 weather classification and support vector machines. *IEEE Trans Ind Appl* 2012;48:1064–9.
1184 doi:10.1109/TIA.2012.2190816.
- 1185 [90] Yona A, Senjyu T, Saber AY, Funabashi T, Sekine H, Kim CH. Application of neural network to one-

- 1186 day-ahead 24 hours generating power forecasting for photovoltaic system. 2007 Int Conf Intell Syst Appl
1187 to Power Syst ISAP 2007:7–12. doi:10.1109/ISAP.2007.4441657.
- 1188 [91] Ding M, Wang L, Bi R. An ANN-based Approach for Forecasting the Power Output of Photovoltaic
1189 System. *Procedia Environ Sci* 2011;11:1308–15. doi:10.1016/j.proenv.2011.12.196.
- 1190 [92] Sfetsos A, Coonick AAH. Univariate and multivariate forecasting of hourly solar radiation with artificial
1191 intelligence techniques. *Sol Energy* 2000;68:169–78. doi:10.1016/S0038-092X(99)00064-X.
- 1192 [93] Mellit A, Kalogirou SA, Shaari S, Salhi H, Hadj Arab A. Methodology for predicting sequences of mean
1193 monthly clearness index and daily solar radiation data in remote areas: Application for sizing a stand-
1194 alone PV system. *Renew Energy* 2008;33:1570–90. doi:10.1016/j.renene.2007.08.006.
- 1195 [94] Raza MQ, Khosravi A. A review on artificial intelligence based load demand forecasting techniques for
1196 smart grid and buildings. *Renew Sustain Energy Rev* 2015;50:1352–72.
- 1197 [95] Taylor JW. An evaluation of methods for very short-term load forecasting using minute-by-minute British
1198 data. *Int J Forecast* 2008;24:645–58. doi:10.1016/j.ijforecast.2008.07.007.
- 1199 [96] Drezga I, Rahman S. Input variable selection for ann-based short-term load forecasting. *IEEE Trans Power*
1200 *Syst* 1998. doi:10.1109/59.736244.
- 1201 [97] Sovann N, Nallagownden P, Baharudin Z. A method to determine the input variable for the neural network
1202 model of the electrical system. 2014 5th Int. Conf. Intell. Adv. Syst. Technol. Converg. Sustain. Futur.
1203 ICIAS 2014 - Proc., 2014. doi:10.1109/ICIAS.2014.6869491.
- 1204 [98] Tao S, Li Y, Xiao X, Yao L. Load forecasting based on short-term correlation clustering. *IEEE Innov.*
1205 *Smart Grid Technol. - Asia*, 2017, p. 1–7. doi:10.1109/ISGT-Asia.2017.8378416.
- 1206 [99] Vinagre E, De Paz JF, Pinto T, Vale Z, Corchado JM, Garcia O. Intelligent energy forecasting based on
1207 the correlation between solar radiation and consumption patterns. 2016 IEEE Symp. Ser. Comput. Intell.
1208 SSCI 2016, 2017. doi:10.1109/SSCI.2016.7849853.
- 1209 [100] Taylor JW. Triple seasonal methods for short-term electricity demand forecasting. *Eur J Oper Res*
1210 2010;204:139–52. doi:10.1016/j.ejor.2009.10.003.
- 1211 [101] Taylor JW, de Menezes LM, McSharry PE. A comparison of univariate methods for forecasting electricity
1212 demand up to a day ahead. *Int J Forecast* 2006;22:1–16. doi:10.1016/j.ijforecast.2005.06.006.
- 1213 [102] Taylor JW, Buizza R. Using weather ensemble predictions in electricity demand forecasting using weather
1214 ensemble predictions in electricity demand forecasting. *Int J Forecast* 2003;19:57–70. doi:10.1016/S0169-
1215 2070(01)00123-6.

- 1216 [103] Gould PG, Koehler AB, Ord JK, Snyder RD, Hyndman RJ, Vahid-Araghi F. Forecasting time series with
1217 multiple seasonal patterns. *Eur J Oper Res* 2008;191:207–22. doi:10.1016/j.ejor.2007.08.024.
- 1218 [104] Al-Hamadi HM, Soliman SA. Short-term electric load forecasting based on Kalman filtering algorithm
1219 with moving window weather and load model. *Electr Power Syst Res* 2004;68:47–59. doi:10.1016/S0378-
1220 7796(03)00150-0.
- 1221 [105] Taylor JW, Mcsharry PE. Short-Term Load Forecasting Methods : An Evaluation Based on European
1222 Data. *IEEE Trans Power Syst* 2008;22:2213–9. doi:10.1109/TPWRS.2007.907583.
- 1223 [106] Villalba SA, Alvarez C. Hybrid demand model for load estimation and short term load forecasting in
1224 distribution electric systems. *Power Deliv IEEE Trans* 2000;15:764–9. doi:10.1109/61.853017.
- 1225 [107] Wang J, Zhu W, Zhang W, Sun D. A trend fixed on firstly and seasonal adjustment model combined with
1226 the ??-SVR for short-term forecasting of electricity demand. *Energy Policy* 2009;37:4901–9.
1227 doi:10.1016/j.enpol.2009.06.046.
- 1228 [108] Zheng Y, Zhu L, Zou X. Short-Term Load Forecasting Based on Gaussian Wavelet SVM. *Energy*
1229 *Procedia* 2011;12:387–93. doi:10.1016/j.egypro.2011.10.052.
- 1230 [109] Badri A, Ameli Z, Motie Birjandi A. Application of Artificial Neural Networks and Fuzzy logic Methods
1231 for Short Term Load Forecasting. *Energy Procedia* 2012;14:1883–8. doi:10.1016/j.egypro.2011.12.1183.
- 1232 [110] Ho K-L, Hsu Y-Y, Chen C-F, Lee T-E, Liang C-C, Lai T-S, et al. Short term load forecasting of Taiwan
1233 power system using a knowledge-based expert system. *IEEE Trans Power Syst* 1990;5:1214–21.
1234 doi:10.1109/59.99372.
- 1235 [111] Galarniotis AI, Tsakoumis AC, Fessas P, Vladov SS, Mladenov VM. Using Elman and FIR neural
1236 networks for short term electric load forecasting. *SCS 2003. Int. Symp. Signals, Circuits Syst. Proc. (Cat.*
1237 *No.03EX720)*, vol. 2, IEEE; 2003, p. 433–6. doi:10.1109/SCS.2003.1227082.
- 1238 [112] Shu F, Luonan C. Short-term load forecasting based on an adaptive hybrid method. *Power Syst IEEE*
1239 *Trans* 2006;21:392–401. doi:10.1109/TPWRS.2005.860944.
- 1240 [113] Zhang B-L, Dong Z-Y. An adaptive neural-wavelet model for short term load forecasting. *Electr Power*
1241 *Syst Res* 2001;59:121–9. doi:10.1016/S0378-7796(01)00138-9.
- 1242 [114] Song K, Baek Y, Hong DH, Jang G. Short-Term Load Forecasting for the Holidays Using. *IEEE Trans*
1243 *Power Syst* 2005;20:96–101. doi:10.1109/TPWRS.2004.835632.
- 1244 [115] Marín FJ, Sandoval F. Short-term peak load forecasting: Statistical methods versus artificial neural
1245 networks. *Lect. Notes Comput. Sci. (including Subser. Lect. Notes Artif. Intell. Lect. Notes*

- 1246 Bioinformatics), 1997. doi:10.1007/BFb0032594.
- 1247 [116] Saber AY, Alam AKMR. Short term load forecasting using multiple linear regression for big data. 2017
1248 IEEE Symp. Ser. Comput. Intell. SSCI 2017 - Proc., 2018. doi:10.1109/SSCI.2017.8285261.
- 1249 [117] Almeshaei E, Soltan H. A methodology for Electric Power Load Forecasting. Alexandria Eng J
1250 2011;50:137–44. doi:10.1016/j.aej.2011.01.015.
- 1251 [118] Bessec M, Fouquau J. Short-run electricity load forecasting with combinations of stationary wavelet
1252 transforms. Eur J Oper Res 2018;264:149–64. doi:10.1016/J.EJOR.2017.05.037.
- 1253 [119] Hong W-C. Hybrid evolutionary algorithms in a SVR-based electric load forecasting model. Int J Electr
1254 Power Energy Syst 2009;31:409–17. doi:10.1016/J.IJEPES.2009.03.020.
- 1255 [120] Yang Y, Li S, Li W, Qu M. Power load probability density forecasting using Gaussian process quantile
1256 regression. Appl Energy 2018;213:499–509. doi:10.1016/J.APENERGY.2017.11.035.
- 1257 [121] Coelho VN, Coelho IM, Coelho BN, Reis AJR, Enayatifar R, Souza MJF, et al. A self-adaptive
1258 evolutionary fuzzy model for load forecasting problems on smart grid environment. Appl Energy
1259 2016;169:567–84. doi:10.1016/J.APENERGY.2016.02.045.
- 1260 [122] Rahman S, Hazim O. A Generalized Knowledge-Based Short-Term Load-Forecasting Technique. IEEE
1261 Trans Power Syst 1993. doi:10.1109/59.260833.
- 1262 [123] Srinivasan D. Parallel neural network-fuzzy expert system strategy for short-term load forecasting :
1263 System implementation and performance evaluation. IEEE Trans Power Syst 1999.
1264 doi:10.1109/59.780934.
- 1265 [124] Hippert HS, Pedreira CE, Souza RC. Neural networks for short-term load forecasting: a review and
1266 evaluation. IEEE Trans Power Syst 2001;16:44–55. doi:10.1109/59.910780.
- 1267 [125] Tsakoumis AC, Vladov SS, Mladenov VM. Electric load forecasting with multilayer perceptron and
1268 Elman neural network. 6th Semin Neural Netw Appl Electr Eng 2002.
1269 doi:10.1109/NEUREL.2002.1057974.
- 1270 [126] Zhang W, Mu G, Yan G, An J. A power load forecast approach based on spatial-temporal clustering of
1271 load data. Concurr Comput Pract Exp n.d.;0:e4386. doi:10.1002/cpe.4386.
- 1272 [127] Hong W-CC. Electric load forecasting by seasonal recurrent SVR (support vector regression) with chaotic
1273 artificial bee colony algorithm. Energy 2011;36:5568–78. doi:10.1016/j.energy.2011.07.015.
- 1274 [128] Dedinec A, Filiposka S, Dedinec A, Kocarev L. Deep belief network based electricity load forecasting:
1275 An analysis of Macedonian case. Energy 2016;115:1688–700. doi:10.1016/j.energy.2016.07.090.

- 1276 [129] Shi H, Xu M, Ma Q, Zhang C, Li R, Li F. A Whole System Assessment of Novel Deep Learning Approach
1277 on Short-Term Load Forecasting. *Energy Procedia* 2017;142:2791–6. doi:10.1016/j.egypro.2017.12.423.
- 1278 [130] Hernandez L, Baladron C, Aguiar J, Carro B, Sanchez-Esguevillas A, Lloret J, et al. A multi-agent system
1279 architecture for smart grid management and forecasting of energy demand in virtual power plants. *IEEE*
1280 *Commun Mag* 2013. doi:10.1109/MCOM.2013.6400446.
- 1281 [131] Javed F, Arshad N, Wallin F, Vassileva I, Dahlquist E. Forecasting for demand response in smart grids:
1282 An analysis on use of anthropologic and structural data and short term multiple loads forecasting. *Appl*
1283 *Energy* 2012. doi:10.1016/j.apenergy.2012.02.027.
- 1284 [132] Hernandez L, Baladron C, Aguiar JM, Carro B, Sanchez-Esguevillas AJ, Lloret J, et al. A survey on
1285 electric power demand forecasting: Future trends in smart grids, microgrids and smart buildings. *IEEE*
1286 *Commun Surv Tutor* 2014. doi:10.1109/SURV.2014.032014.00094.
- 1287 [133] Nowotarski J, Weron R. Recent advances in electricity price forecasting: A review of probabilistic
1288 forecasting. *Renew Sustain Energy Rev* 2018;81:1548–68.
- 1289 [134] Weron R. Electricity price forecasting: A review of the state-of-the-art with a look into the future. vol. 30.
1290 2014. doi:10.1016/j.ijforecast.2014.08.008.
- 1291 [135] Yang Z, Ce L, Lian L. Electricity price forecasting by a hybrid model, combining wavelet transform,
1292 ARMA and kernel-based extreme learning machine methods. *Appl Energy* 2017;190:291–305.
1293 doi:10.1016/j.apenergy.2016.12.130.
- 1294 [136] Abedinia O, Amjady N, Shafie-Khah M, Catalão JPSPS. Electricity price forecast using Combinatorial
1295 Neural Network trained by a new stochastic search method. *Energy Convers Manag* 2015;105:642–54.
- 1296 [137] Wang D, Luo H, Grunder O, Lin Y, Guo H. Multi-step ahead electricity price forecasting using a hybrid
1297 model based on two-layer decomposition technique and BP neural network optimized by firefly algorithm.
1298 *Appl Energy* 2017;190:390–407. doi:10.1016/J.APENERGY.2016.12.134.
- 1299 [138] Amjady N, Daraeepour A. Mixed price and load forecasting of electricity markets by a new iterative
1300 prediction method. *Electr Power Syst Res* 2009;79:1329–36. doi:10.1016/J.EPSR.2009.04.006.
- 1301 [139] Ghasemi A, Shayeghi H, Moradzadeh M, Nooshyar M. A novel hybrid algorithm for electricity price and
1302 load forecasting in smart grids with demand-side management. *Appl Energy* 2016;177:40–59.
- 1303 [140] Hong T, Fan S. Probabilistic electric load forecasting: A tutorial review. *Int J Forecast* 2016;32:914–38.
1304 doi:10.1016/j.ijforecast.2015.11.011.
- 1305 [141] Zhang Y, Wang J, Wang X. Review on probabilistic forecasting of wind power generation. *Renew Sustain*

- 1306 Energy Rev 2014;32:255–70. doi:10.1016/j.rser.2014.01.033.
- 1307 [142] van der Meer DW, Widén J, Munkhammar J. Review on probabilistic forecasting of photovoltaic power
1308 production and electricity consumption. *Renew Sustain Energy Rev* 2018;81:1484–512.
1309 doi:10.1016/j.rser.2017.05.212.
- 1310 [143] Peng Y, Rysanek A, Nagy Z, Schlüter A. Using machine learning techniques for occupancy-prediction-
1311 based cooling control in office buildings. *Appl Energy* 2018;211:1343–58.
1312 doi:10.1016/J.APENERGY.2017.12.002.
- 1313 [144] Zahid T, Xu K, Li W, Li C, Li H. State of charge estimation for electric vehicle power battery using
1314 advanced machine learning algorithm under diversified drive cycles. *Energy* 2018;162:871–82.
1315 doi:10.1016/J.ENERGY.2018.08.071.
- 1316 [145] Fu X, Zhang X. Estimation of building energy consumption using weather information derived from
1317 photovoltaic power plants. *Renew Energy* 2019;130:130–8. doi:10.1016/J.RENENE.2018.06.069.
- 1318 [146] Saloux E, Candanedo JA. Forecasting District Heating Demand using Machine Learning Algorithms.
1319 *Energy Procedia* 2018;149:59–68. doi:10.1016/J.EGYPRO.2018.08.169.
- 1320 [147] Tomin N V., Kurbatsky VG, Sidorov DN, Zhukov A V. Machine Learning Techniques for Power System
1321 Security Assessment. *IFAC-PapersOnLine* 2016;49:445–50. doi:10.1016/J.IFACOL.2016.10.773.
- 1322 [148] Karim M Al, Currie J, Lie T-T. A machine learning based optimized energy dispatching scheme for
1323 restoring a hybrid microgrid. *Electr Power Syst Res* 2018;155:206–15. doi:10.1016/J.EPSR.2017.10.015.
- 1324 [149] Staffell I, Pfenninger S. *Renewables.ninja* 2015.
- 1325 [150] Staffell I. *Wind Turbine Power Curves* 2012:1–6.
- 1326 [151] Staffell I, Green R. How does wind farm performance decline with age ? *Renew Energy* 2014;66:775–86.
1327 doi:10.1016/j.renene.2013.10.041.
- 1328 [152] Yang J, Leskovec J. Patterns of Temporal Variation in Online Media. *Time* 2011;468:177–186.
1329 doi:10.1145/1935826.1935863.
- 1330 [153] Kalogirou S a. Artificial neural networks in renewable energy systems applications: a review. *Renew*
1331 *Sustain Energy Rev* 2001;5:373–401. doi:10.1016/S1364-0321(01)00006-5.
- 1332 [154] Soman PC. *An Adaptive NARX Neural Network Approach for Financial Time Series Prediction*. 2008.
- 1333 [155] Lin T, Horne BG, Tiño P, Giles CL. Learning long-term dependencies in NARX recurrent neural
1334 networks. *IEEE Trans Neural Networks* 1996;7:1329–38. doi:10.1109/72.548162.
- 1335 [156] Xie H, Tang H, Liao YH. Time series prediction based on narx neural networks: An advanced approach.

- 1336 Proc 2009 Int Conf Mach Learn Cybern 2009;3:1275–9. doi:10.1109/ICMLC.2009.5212326.
- 1337 [157] Li Z, Best M. Structure optimisation of input layer for feed-forward NARX neural network. Int J Model
1338 Identif Control 2016;25:217. doi:10.1504/IJMIC.2016.075814.
- 1339 [158] Tao C, Shanxu D, Changsong C. Forecasting power output for grid-connected photovoltaic power system
1340 without using solar radiation measurement. 2nd IEEE Int Symp Power Electron Distrib Gener Syst
1341 2010:773–7. doi:10.1109/PEDG.2010.5545754.
- 1342 [159] Siegelmann HT, Horne BG, Giles CL. Computational capabilities of recurrent NARX neural networks.
1343 IEEE Trans Syst Man, Cybern Part B Cybern 1997;27:208–15. doi:10.1109/3477.558801.
- 1344 [160] Hornik K. Approximation capabilities of multilayer feedforward networks. Neural Networks 1991;4:251–
1345 7. doi:10.1016/0893-6080(91)90009-T.
- 1346 [161] Cybenko G. Correction: Approximation by Superpositions of a Sigmoidal Function. Math Control
1347 Signals, Syst 1989;2:303–14. doi:doi: 10.1007/BF02134016.
- 1348 [162] Erb RJ. Introduction to Backpropagation Neural Network Computation. Pharm Res An Off J Am Assoc
1349 Pharm Sci 1993;10:165–70. doi:10.1023/A:1018966222807.
- 1350 [163] Beale MH, Hagan MT, Demuth HB. Neural Network Toolbox™ User’s Guide with MATLAB. 2015.
1351 doi:10.1016/j.neunet.2005.10.002.
- 1352 [164] Wu X, Kumar V, Ross Quinlan J, Ghosh J, Yang Q, Motoda H, et al. Top 10 algorithms in data mining.
1353 vol. 14. 2008. doi:10.1007/s10115-007-0114-2.
- 1354 [165] Sayad S. Real Time Data Mining. Self-Help Publishers; 2011.
- 1355 [166] Cortes C, Vapnik V. Support-vector networks. Mach Learn 1995;20:273–97. doi:10.1007/BF00994018.
- 1356 [167] Suykens J, Van Gestel T, De Brabanter J, De Moor B, Vandewalle J. Least Squares-Support Vector
1357 Machines, Toolbox for Matlab/C v1.8 2011.
- 1358 [168] Suykens J, Van Gestel T, De Brabanter J, Vandewalle J. Least Squares Support Vector Machines.
1359 Singapore: World Scientific; 2002.
- 1360 [169] Rasmussen CE, Williams CKI. Gaussian processes for machine learning. vol. 14. MIT Press; 2006.
1361 doi:10.1142/S0129065704001899.
- 1362 [170] Kocijan J, Ažman K, Grancarova A. The concept for Gaussian process model based system identification
1363 toolbox. Proc 2007 Int Conf Comput Syst Technol - CompSysTech '07 2007:1.
1364 doi:10.1145/1330598.1330647.
- 1365 [171] Greiger A. Gaussian Processes for Machine Learning. An introduction to Gaussian Processes, (scaled)

- 1366 GPLVMs, (balanced) GPDMs and their applications to 3D people tracking, 2007.
- 1367 [172] Stepančić M, Kocijan J. Gaussian-Process-Model-based System-Identification Toolbox for Matlab,
1368 GPdyn. n.d.
- 1369 [173] Sharifzadeh M, Lubiano-Walochik H, Shah N. Integrated renewable electricity generation considering
1370 uncertainties: The UK roadmap to 50% power generation from wind and solar energies. *Renew Sustain*
1371 *Energy Rev* 2017;72:385–98. doi:10.1016/j.rser.2017.01.069.
- 1372 [174] BEIS. Digest of UK Energy Statistics (DUKES): renewable sources of energy. DUKES chapter 6:
1373 statistics on energy from renewable sources. UK National Statistics 2018.
- 1374 [175] Intertek Testing & Certification Ltd. Household electricity survey. A study of domestic electrical product
1375 usage. 2012.
- 1376 [176] Kennel F, Gorges D, Liu S. Energy Management for Smart Grids With Electric Vehicles Based on
1377 Hierarchical MPC. *Ind Informatics, IEEE Trans* 2013;9:1528–37. doi:10.1109/TII.2012.2228876.
- 1378
- 1379